

# **Design of a system to study the adhesive properties of nanoscopic ice layers at cryogenic temperatures**

---

Master thesis by Linnea Widmayer  
Date of submission: October 2, 2023

Supervisor: Prof. Thomas Burg  
Reviewer: Niko Faul  
Darmstadt



TECHNISCHE  
UNIVERSITÄT  
DARMSTADT

Electrical Engineering and  
Information Technology  
Department  
IMNS

---

## **Erklärung zur Abschlussarbeit gemäß § 22 Abs. 7 APB TU Darmstadt**

Hiermit erkläre ich, Linnea Widmayer, dass ich die vorliegende Arbeit gemäß § 22 Abs. 7 APB der TU Darmstadt selbstständig, ohne Hilfe Dritter und nur mit den angegebenen Quellen und Hilfsmitteln angefertigt habe. Ich habe mit Ausnahme der zitierten Literatur und anderer in der Arbeit genannter Quellen keine fremden Hilfsmittel benutzt. Die von mir bei der Anfertigung dieser wissenschaftlichen Arbeit wörtlich oder inhaltlich benutzte Literatur und alle anderen Quellen habe ich im Text deutlich gekennzeichnet und gesondert aufgeführt. Dies gilt auch für Quellen oder Hilfsmittel aus dem Internet.

Diese Arbeit hat in gleicher oder ähnlicher Form noch keiner Prüfungsbehörde vorgelegen.

Mir ist bekannt, dass im Falle eines Plagiats (§ 38 Abs. 2 APB) ein Täuschungsversuch vorliegt, der dazu führt, dass die Arbeit mit 5,0 bewertet und damit ein Prüfungsversuch verbraucht wird. Abschlussarbeiten dürfen nur einmal wiederholt werden.

Bei einer Thesis des Fachbereichs Architektur entspricht die eingereichte elektronische Fassung dem vorgestellten Modell und den vorgelegten Plänen.

Darmstadt, 2. Oktober 2023

---

L. Widmayer

# Acknowledgment

---

First I want to thank Prof. Thomas Burg for his advice and support. My gratitude goes to Nico Faul for his guidance throughout my whole master thesis. Last I want to thank my family, partner and friends for motivation and support especially in the writing process of this thesis.

# Abstract

---

Light microscopy and electron microscopy are both widely used tools to study samples. Light microscopy makes detailed observation possible with visible light. Additionally, fluorescence can be used to highlight certain areas of interest within a sample. In electron microscopy, structures to the sub-nanometer is made visible by using a focused electron beam. The distribution of different atoms is also observable. The strengths of both microscopy methods complement each other in analysis.

As both microscopy methods are fundamentally different, sample preparation fulfill different conditions to enable good visibility in according microscopy method. Still in cryo microscopy, both use similar preparation steps. In both a vitrified ice is created to fixate the specimen inside an ice layer on the sample holder. The sample holder are designed to enable the applied microscopy method. Therefore, examining the sample in cryo-microscopy is limited by sample holder design.

In this master thesis, methods to switch sample holders at cryogenic temperatures are investigated. An additional layer is designed between sample holder and ice layer to enable detachment. Two different approaches of layer design are explored: Using a sacrificial layer to separate the ice containing the specimen and reducing adhesion of the ice layer to the sample holder to make mechanical separation possible.

To design a sacrificial layers, lipids are investigated. In theory, solvents are dissolving the sacrificial lipid layer at cryogenic temperatures. The sample holder is coated in parylene to decrease adhesion of ice and avoid (re-) attachment after dissolving. Solvents are tested regarding solubility at room temperature and around  $-140^{\circ}\text{C}$ . Results show that dissolving lipids is generally an endothermic process. Dissolving a DOPC and EGG-PC lipid layer at cryogenic temperatures is possible but not applicable for dissolving a sacrificial layer.

To be able to mechanically lift off the ice layer without destroying the specimen, multiple assemblies are used. A lifting assembly named "finger" uses the temperature dependent viscosity of Hydrofluorether to attach and detach to the ice layer. Baths filled with liquid nitrogen are used for cooling and sample preparation. An inverted fluorescence microscope with a cryo-stage is used to confirm successful detachment.

At room temperature, PDMS is tuned to reduce adhesion. The effect of plasma treatment is researched by tensile testing on 1:2 base coat to curing agent ratio. The results show an increase of tensile strength of PDMS of up to 6 fold of untreated PDMS. On the other hand, this is not the case for mixture ratio with higher base coat content. The PDMS layer gets brittle and reduces adhesion in that way.

At cryogenic temperatures, sample holders coated with plasma treated PDMS and Parylene/lipids are compared to each other. Breaking the ice layer is successful in  $\frac{1}{4}$  th of cases with Parylene/lipid coated sample holders. A successful detachment was archived once with a sample holder coated with PDMS mixture ratio of 4:1.

Future work could focus on increasing solubility of lipids and other detergents by tuning pH-value. Also other methods for loosening the ice layer should be investigated.

# Contents

---

<b>1</b>	<b>Introduction</b>	<b>6</b>
1.1	Task and requirements . . . . .	7
1.2	State-of-the-art . . . . .	7
<b>2</b>	<b>Concept</b>	<b>10</b>
2.1	Dissolving Phospholipids . . . . .	10
2.2	Separating the ice layer mechanically . . . . .	11
<b>3</b>	<b>Solubility lipids</b>	<b>13</b>
3.1	Preparation of lipid coated slides . . . . .	14
3.1.1	at room temperature . . . . .	14
3.1.2	at cryogenic temperature . . . . .	15
<b>4</b>	<b>Separating ice layer mechanically</b>	<b>17</b>
4.1	PDMS experiments at room temperature . . . . .	17
4.1.1	Preparation of PDMS samples . . . . .	18
4.1.2	Setup of the pulling machine . . . . .	19
4.1.3	Tensile testing of PDMS . . . . .	20
4.1.4	Visible changes of 50:1 mixture ratio PDMS with plasma activation . . . . .	24
4.2	Experiments at cryogenic temperature . . . . .	24
4.2.1	Preparation of samples . . . . .	25
4.2.2	Inverted microscope . . . . .	26
4.2.3	Baths . . . . .	27
4.2.4	Finger . . . . .	29
4.2.5	Setup pulling machine for cryogenic tests . . . . .	31
4.2.6	Factors observed influencing detachment with finger . . . . .	32
4.2.7	Tensile testing of engineered layer with finger . . . . .	38
<b>5</b>	<b>Conclusion and Outlook</b>	<b>45</b>
<b>6</b>	<b>References</b>	<b>47</b>

# 1 Introduction

---

Light microscopy (LM) is the simplest and most commonly used to magnify small objects and structures. There are many building varieties for different applications with different magnification ranges. In general, two building variation exist: Transmission LM do let light pass through the sample to create an image. Reflective LM uses the reflecting light from the sample for imaging.

For example, some light microscopes have additional fluorescence filters to detect fluorescence signals. These filters allow only the specific wave length emitted by a fluorescent molecule to pass. As a light source, filtered white light and lasers can be used, since only a specific wavelength range excites fluorescent molecules.

In LM many new advancements are still made. The Abbe criterium is the major limit for many light microscopes. However, multiple modified LM methods exist which are able to increase the resolution beyond this limit [1].

Electron microscopy (EM) is another imaging method being used: With electrons, resolutions down to the size of atoms are possible. The smallest structures in sub nanometer scale are observable with this method. Even the distribution of certain elements is detectable. Also the creation of 3D images are possible.

In EM, water containing structures must be fixated. One way to archive fixation of the specimen is to freeze the water to ice at cryogenic temperatures. With rapid cooling below  $-120^{\circ}\text{C}$  within tenths of milliseconds, vitrified ice which is amorphic and does not destroy structures by forming ice crystals is reached [2]. This requires low thermal conductivity which is only achievable with small and well thermal conducting sample holders. To hold the ice structure, all setups including microscopes to handle the specimen needs to be cooled below  $-120^{\circ}\text{C}$  to prevent subsequent crystallization of the ice.

To reach transparency of the electron beam for cryo scanning electron microscopy (cryo-TEM), the sample is required to have a maximum thickness of 100 nm and containing only lighter elements. Additionally, a thin film in combination of a metal grid is used as a sample holder [3]. This grid does not deliver a regular background. Additionally, the sample needs to have low absorption of light in the visible spectrum in case a laser being used. If the contrast is too high, the sample is damaged through light absorption and resulting heat.

For cryo-LM, the thin ice layer is frozen onto a thin sapphire disk. also here the thickness is limited by thermal conductivity to reach the vitrified state. The surface needs to be transparent in visible light or with low contrast [4].

Conveniently, the process of sample preparation for cryo-LM and cryo-EM is very similar. Still, the sample holder used for LM and EM are very limited inter operable. This grid does not deliver a regular background for reflective EM. Also a grid is not completely transparent for light for transmissive LM. also the grid absorbs visible light, limiting the use of lasers. The slides used in LM are mostly too thick for EM. Sometimes heavier elements are used too. Additionally some form of metal grid must be added for EM.

Nevertheless, combining LM and EM on the same sample brings big advantages: The larger scale of LM and the use of multiple wavelengths combined with fluorescence and high resolution on the same sample does make studying samples easier. In this master thesis, a method for using cryo ILM and cryo-EM on the

same sample is examined. To make this possible, the sample must be transferred to different sample holders between cryo-LM and cryo-EM without destroying the sample. To achieve this, a layer between ice and sample holder is engineered to enable detachment and transfer to another sample holder (Fig. 1.1).

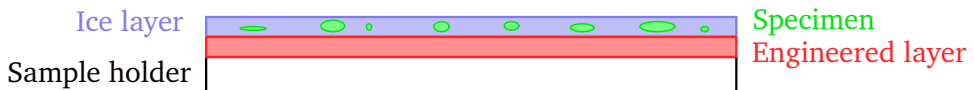


Figure 1.1: Depiction of a sample. The specimen is frozen inside the ice layer. The sample holder and ice layer are connected by an additional engineered layer. In this master thesis, the additional layer is varied to allow separation of the ice including the specimen from the sample holder.

## 1.1 Task and requirements

There are several requirements for this engineered layer: The layer must be thin to keep thermal conductivity high at freezing. The layer also must be hydrophilic and even to enable freezing a regular thin ice layer on top. The engineered layer should not disturb LM or EM.

The order of which kind of microscopy is performed first has an influence on the design of the layer. As the thickness and the design of the sample holder is less restrictive at LM, designing the layer for this environment is also easier. Therefore, LM is performed first in the final process. Then the ice layer is transferred to a grid. After this, cryo-EM is performed.

There are several challenges to perform a sample holder change: First, high wettability is needed when plunge-freezing. Wettability highly increases adhesion of ice on the rest of the sample. Second, the engineered layer is thin and covered by ice and sample holder. Therefore access to the layer is limited by solvents or other liquids. Third, the ice layer must stay in a vitrified state in the whole process. Last, many characteristics are temperature dependent. Results of experiments done at room temperature or close to freezing point are not easily transferable at  $-140^{\circ}\text{C}$ . For example, even mechanical stability and adhesion forces of all layers varies over temperature. Therefore everything needs to be validated at cryogenic temperatures [5].

To fulfill all the requirements, following ideas are pursued. A sacrificial layer between sample holder and ice could be dissolved. The ice layer will float separately in the solution and could then be transferred to another sample holder. The second idea is to mechanically separate a piece or the hole ice layer from the sample holder. The layer must be designed in a way to reduce adhesion and posses high wettability at the same time. Also the forces applied must be strong enough for separation.

## 1.2 State-of-the-art

Ice removal is needed in multiple commercial applications. Most strategies are only applicable in temperatures down to  $-30^{\circ}\text{C}$ . Since the ice layer in the demonstrated application needs to stay vitrified at under  $-140^{\circ}\text{C}$  or even lower, only few anti-frosting methods are feasible. For example the active anti-frosting strategy of heating the ice is not possible, as the specimen must stay contained within the ice layer.

There are four passive anti-frosting strategies: Inhibition of ice nucleation is achieved by using surface inherent properties to prevent ice crystals from forming. Retardation of frosting removes water to prevent icing on the

surface with water repellent properties such as the lotus effect. Mitigation of frost accumulation prevents already formed ice droplets from further accumulating and forming an ice layer. Last a reduction of ice adhesion on the surface prevents ice droplets to stay on the surface. Other forces like wind or gravity removes ice droplets and keeps the surface ice free [6].

Out of the four passive anti-frosting strategies, only one is applicable at cryogenic temperatures. The reduction of ice adhesion can be used to decrease the force needed to separate the ice layer mechanically. This can be done by using a hydrophobic surface with general low adhesion or with surface structuring. In contrast, Inhibition of ice nucleation, retardation of frosting and mitigation of accumulation only inhibit the freezing process itself and are therefore not applicable.

In industrial application, one commonly used coating to reduce adhesion of ice is Polydimethylsiloxane (PDMS). PDMS is a polymer which is widely used in different applications like in fabrication of micro channels, chip manufacturing, aerospace industry and medical tools. PDMS properties are for example its hydrophobicity, biocompatibility and electric insulating capabilities. Also PDMS is cost effective and allows rapid prototyping, molding and thin coatings [7]. Additionally, PDMS is modifiable with additives.

One example in which the low ice adhesion potential of PDMS is illustrated is the passive deicing of Aircrafts in flight. As ice can influence the air flow around the wing an the body, which induces turbulence and reduces lift. Ice protection is therefore critical for a save and stable flying. In [8], PDMS is tuned for optimal characteristics in flight. To test the surfaces, flight conditions of 0.5 bar and  $-12^{\circ}\text{C}$  are simulated. Fluorinated PDMS with and without silica nanoparticles are compared to aluminum, showing better resistance against ice growth. The different coatings are also examined regarding contact angle of water and surface roughness. Also the stability of the surface is relevant as ice formation and impacts can also wear down the coating itself.

To create PDMS surfaces in labs Dowsil Sylgard 184 Silicone elastomer is widely used[9]. The PDMS kit includes a curing agent and base coat component. The specified mixture ratio is 10 base coat to 1 curing agent in weight (10:1). In some applications, other mixture ratios are used and additives are added for tuning PDMS.

For example, adhesion forces of ice on PDMS varies with different mixture ratios. In [10], PDMS is investigated in 3:1 to 1:50 weight ratio. The mixture is given into a mold and afterwards fully cured. An ice block is frozen on top of the PDMS. Using a pulling machine the maximum tensile and shear forces for detaching ice from PDMS are determined. Results show that mixture ratios 10:1 to 1:3 have significant lower adhesion forces on ice. At for example at 2:1, the shear mode is just under 20 kPa and the tensile mode around 30 kPa.

Plasma curing is commonly used as PDMS treatment. Plasma treatment used for increasing wettability and adhesion. Plasma treatment is changing the chemistry of the polymer chains on the surface. Charged Oxygen Ions are deposited on the surface. these Ions make the surface temporarily hydrophile and increasing water adhesion. The Ions change the structure of the PDMS is permanently by oxidation. In some cases, cracks form as the surface oxidizes to a silica like form.

In [11], the influence of different gasses on PDMS plasma treatment are examined. Oxygen, Nitrogen, Argon and Helium are compared on the effect on wettability, adhesion and cracking. Thin PDMS sheets are used with unknown composition. They found similar results between gasses. All gasses produced a thin and brittle surface with cracks and high wettability. Based on these results, used gas is not a significant factor for plasma activation. Therefore using only air (mainly a mixture of nitrogen and oxygen) is sufficient to determine the effect of plasma treatment.

In [12], the influence of plasma treatment on Mixture ratios of 50:1 to 100:1 is described. A thin layer of those PDMS mixtures is put onto a preformed PDMS piece with lower mixture ratio. The preformed piece is

used to apply shear stress to the surface by stretching the lower PDMS form piece. Therefore only tensile force are examined. It shows no significant difference between described mixture ratios. It also shows that higher plasma treatment leads to more brittle surfaces, reducing the force needed to break the PDMS Layer by 90%.

PDMS properties are also temperature dependent. In [21], multiple characteristics are determined for cryogenic temperatures. The PDMS is prepared with the standard mixture ratio of 10:1. The compressive strength increases with lower temperatures until  $-123.15^{\circ}\text{C}$ . At this temperature, the compressive strength reaches a maximum of 224.50 MPa in average. At lower temperatures, the PDMS gets brittle. At  $-150.15^{\circ}\text{C}$  PDMS has a compressive strength of 106.99 MPa.

## 2 Concept

To detach the ice layer from the sample holder, two main ideas are proposed: The first is using mechanical force to separate the ice layer. The second idea is designing a sacrificial layer which can be dissolved at cryogenic temperatures. In this chapter, the concept and procedure of each method is explained.

### 2.1 Dissolving Phospholipids

Phospholipids are made of two long non-polar carbon chains and a polar head. A membrane is a bilayer of Phospholipids with the hydrophobic carbon chains oriented inwards and the hydrophilic head pointing outwards. They are also natural detergents, as they can bind to hydrophobic waste forming an emulsion, making them removable with polar liquids like water [13].

As Lipids are dissolvable at common solvents at room temperature, the idea is to use lipids as sacrificial layer at cryogenic temperatures. A solvent is used to dissolve the sacrificial lipid layer. To make this possible, a solvent with high solubility of lipids at cryogenic temperatures must be found. As the dissolving process is temperature dependent, solvents at room temperature are not necessarily solvents at cryogenic temperatures. Experiments are conducted to find a solvent to dissolve a lipid layer at cryogenic temperatures.

Parylene is a hydrophobic polymer used as a coating to repel particles, including water and ice. Parylene is also bio compatible and used in medicine and biology [14]. Parylene is not usable without a second layer on top. Parylene hydrophobicity does not allow water to spread during plunge freezing. With plasma activation, the surface is now hyrdophilic, but ice adheres to the parylene too strong for mechanical separation.

For this reason, lipids are used in combination with parylene (Fig. 2.1). The hydrophobic chains of the lipids adhere to the parylene. The polar head allow water to spread evenly over the surface. Solving the lipids with a solvent will detach the ice layer from the sample holder. Parylene additionally prevents (re-) attachment through holes in the lipid layer.

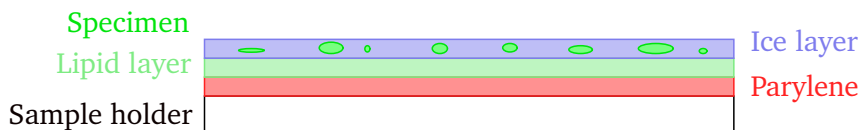


Figure 2.1: Layers of a sample. The lipid layer is used as a sacrificial layer. To reach the layer with a solvent, the only contact surface is to the edge. To get a fast and reliable process, a solvent with high solubility is needed.

## 2.2 Separating the ice layer mechanically

The other method discussed is to mechanically lift a part or the whole ice layer from the sample holder it is frozen to. The sample is frozen with plunge-freezing. For later steps the sample is prepared in a bath. The "finger" assembly is used to attach and pull on the ice layer. Hydrofluorether (HFE) temperature dependent viscosity is used to connect and pull onto the ice layer with the finger.

The goal is to vary the engineered layer do reduce the adhesion between ice and sample holder. The parylene and lipid coated samples are tested regarding being separable with the finger. Additionally, PDMS is used for its general low adhesion to ice (Fig. 2.2). To freeze a thin ice layer on top, the PDMS is plasma activated.

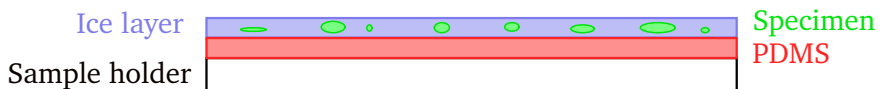


Figure 2.2: Sample holder coated with PDMS. With plasma activation and changing mixture ratio of the PDMS, low adhesion is pursued.

With different mixture ratios and plasma treatment, PDMS is tuned to be hydrophile at freezing and keeping low adhesion when separating. It is hydrophobic and has a low surface energy. It can be coat spinned into a thin layer on top of the sample holder. Also it is widely available and tunable. To use PDMS in plunge freezing, PDMS is plasma activated.

To create different PDMS mixtures, Dowsil Sylgard 184 Silicone elastomer is used[9]. In this master thesis, I focus on tuning PDMS by changing mixture ratio of base coat to curing agent to reduce adhesion of the ice layer to the sample holder. For tuning tensile testing is performed at room temperature to determine the effect of plasma activation and PDMS mixture ratio.

Tensile testing is done on PDMS coated cover glass pieces with a tensile testing machine. A stamp is glued on top of the PDMS layer with UV-glue. The stamp is pulled up by the tensile testing machine while the cover glass piece is clamped to the stationary bottom side. With the maximum force and area left behind by the UV-glue, the tensile stress is determined.

First, different mixture ratios and a control uncoated cover glass is compared. Then, the effect of plasma curing is tested on PDMS at mixture ratios with low base coat portion. With these results, a mixture ratio with low adhesion is found to test at cryogenic temperatures.

To test the effect of the engineered layer at cryogenic temperatures, a small bath filled with liquid nitrogen is placed below the finger. In the bath, samples are prepared. It additionally contains a harbor-shuttle system. The sample is fixed to the shuttle for transportation and fixation for tests with the finger. A warm nitrogen gas barrier keeps the finger tip and the content of the bath ice free by displacing humid air.

To try out the separating with the finger in a repeatable manner, following process is used: The sample is plunge-frozen with water mixed with fluoresceine or taken out of the storage and placed on the work surface in the bath. The sample is fixed to a copper shuttle. The now prepared shuttle is transported quickly to the microscope for pre-imaging. After microscopy, the sample is placed into the bath under the cooled finger. HFE is applied to the tip. The finger is lowered onto the sample in "unglue" mode. Lowering and correction of position is done with three stages until the HFE contacts and spreads over the sample. The temperature is reduced to "glue" temperature and waited until the sample and finger is cooled down. When the temperature is reached the finger is pulled up by turning one stage until detachment. Then the shuttle is transported to the microscope and the sample is analyzed.

When detachment is successful, the ice piece hanging on the finger is placed on another shuttle. This is done by lowering the finger onto a new sample holder fixed onto another shuttle and raising the Temperature to "unglue" mode.

The finger is also combined tensile testing machine. The finger is fixed to the top, while the bath is fixed to the bottom. The force at separation can be measured and quantified. The tensile strength of HFE can also be estimated. These results can be compared to data collected at pulling tests at room temperature and data in papers.

As the finger is used for this application for the first time, different variables are determined which could significantly influence successful detaching. With experiments, these variables are examined to improve the reliability of the finger. Following main variables are determined: The right volume of HFE on finger tip improves reliability. The temperature influences the strength of HFE. The right direction of force can make separation easier. Right positioning is important to induce forces efficient onto the right surfaces.

## 3 Solubility lipids

---

Lipids are chosen because they possess a hydrophobic and hydrophilic part. They can hold an ice layer onto a hydrophobic sample holder without any other modifications which could increase adhesion. Also, lipids are dissolvable in common solvents which are liquid at cryogenic temperatures. Therefore, dissolving lipids at cryogenic temperatures to separate the ice layer would be a practical and gentle way to separate the ice layer. To test this theory, a strong enough solubility of Lipids at cryogenic temperatures must be proven first.

Solubility is temperature dependent. The process of dissolving a solute in a solvent can be virtually broken down into three steps: First, the structure of the solute must be broken up with energy. Second the structure of the solvent is also broken up also using energy. Last, the solute and solvent are rearranged into a new structure which releases energy. Depending on the ratio of energy used by breaking the structure of solute and solvent and the energy released at rearranging, the process is more or less endo- or exothermic [15]. Exothermic processes have higher solubility at low temperatures, while Endothermic processes have higher solubility at high temperatures [16].

A quick look at the chemical structure of lipids reveals that solving lipids is most likely endothermic. lipids ordered in layers are held together with Van-der-vaals forces, hydrogen bindings and electrostatic bonds [17]. Also in a layer, each lipid is bond to several surrounding lipids. This results in a very strong bond to break up when dissolving. Therefore, a high amount of energy is needed to break up the lipid layer structure.

For dissolving lipids at cryogenic temperatures, exothermic processes are favorable. Still, exothermic processes release energy in form of heat, which can damage the ice layer when heated up too much. Therefore, a mostly neutral dissolving process is optimal.

Additionally, some solvents tested are soluble in water. It is unknown whether the solvents could be solved or diffuse inside the ice layer at  $-140^{\circ}\text{C}$ . Therefore the ice layer could be changed in some undesired manner. if a sufficient solvent is found and the solvent is soluble in water, a potential change of the vitrified ice needs to be addressed.

Tests are conducted to find a solvent to dissolve a sacrificial layer out of lipids. Two consecutive solubility experiments are proposed. The first experiment is conducted at room temperature. the aim is to find solvents with high solubility at room temperature. the candidates with high solubility are then tested in the next experiment at cryogenic temperature. the aim is now to find solvents with also high solubility at cryogenic temperatures. The first experiment is conducted as there are only three baths available at cryogenic temperature. therefore the throughput for experiments is limited. All tests are conducted on lipid and parylene coated sample holders.

### **3.1 Preparation of lipid coated slides**

Two different kind of lipids are used: DOPC and EGG-PC. DOPC is stored as a powder. The DOPC powder is dissolved in Ethanol (25 mg/1 mL lipid to solvent) for application. EGG-PC is shipped solved in chloroform in two different ratios: 25 mg/1 mL and 10 mg/1 mL. The solution is shipped in vials.

The solution containing lipids is transferred into several small bottles. They are chosen over a big bottle because solution forms a lubricating film on the thread of the lid. This film prevents the lid from closing airtight. non airtight bottles lead to evaporation of the solvent over time, changing and destroying the solution inside. In the coating process, solution often drops onto the threads, making a bottle only usable in one coating session. By splitting the solution into multiple bottles, more slides can be covered by one batch of lipid containing solution.

The solubility of lipids is tested on coated sample holders without the ice layer. A round Ø5 mm cover glass is chosen as sample holder as cheap substitute. The cover glass is coated with a thin layer of parylene. The coated cover glass is dipped into lipid solution. Then the coated cover glass is dried, leaving behind a lipid layer on the parylene. After preparation, streaks are visible on the sample holder which indicate the presence of lipids forming an irregular lipid layer (Fig. 3.1). The prepared sample holders are then used in solubility experiments.



Figure 3.1: Example of a Ø5 mm cover glass with streaks of lipid residuals on the surface.

#### **3.1.1 at room temperature**

Solvents tested for dissolving the sacrificial layer are chosen based on availability, freezing point and safety. These solvents are readily available in the laboratory. Some are ordered before the test. All chosen solvent need to be safe to use in a well ventilated room. The dissolving cannot be conducted under a extractor hood as too much space is taken up with the experiment. Also the solvent needs to stay liquid at around -140 °C to assure that the ice layer on top stays vitrified. The tested substances are 4-Methyl Pentene, 3-Methyl Pentene, 1-Pentene, Isopentane, 1-Propanol, Pentane and Ethanol.

The solubility of lipids in different solvents are determined at room temperature first. For this experiment, the sample holders are prepared as described before. Then a first reference image was taken. The cover glass is given into a small container with the solvent candidate. After 15 minutes, the sample holder is removed and compared under the microscope with the reference picture. If streaks created from lipids are still as visible as before, the lipids are categorized as insoluble in this solvent. If the streaks partially disappeared and/or are less visible, the lipids are categorized as partially soluble in this solvent. Last if the streaks completely disappear, the lipids are assigned as soluble in the solvent (Table 3.1).

potential solvent	solubility EGG-PC	solubility DOPC
4-Methyl Pentene	soluble	N/A
3-Methyl Pentene	slightly soluble	insoluble
1-Pentene	insoluble	insoluble
Isopentane	soluble	slightly soluble
1-Propanol	soluble	soluble
Pentane	soluble	insoluble
Ethanol	N/A	soluble

Table 3.1: Result of solubility tests at room temperature. Soluble indicates solvents which are able to visibly dissolve all lipids off a sample holder. slightly soluble indicates solvents which are able to dissolve lipids with residuals. Insoluble indicates no visible removal of lipid residuals on a sample holder.

This experiment shows that three different solvent exist for each EGG-PC and DOPC with high solubility (Table 3.1). Following these results, solvents categorized with "soluble" are tested regarding solubility at temperatures of  $-140\text{ }^{\circ}\text{C}$ .

### 3.1.2 at cryogenic temperature

The experiment process is nearly the same as at room temperature, except dissolving is conducted at  $-140\text{ }^{\circ}\text{C}$ . The solvents are given in baths cooled with liquid nitrogen, which are regulated to the desired temperature. A lipid coated slide is given into the cold solvent for 15 min. Then the slide is examined for leftover streaks as before.

As not all solvents are liquid at  $-140\text{ }^{\circ}\text{C}$  (Table 3.2), they are tested at higher temperatures above their melting point. In addition they are tested as mixtures with other solvents with a lower melting point. Additionally liquid ethane is tested only at  $-140\text{ }^{\circ}\text{C}$ . Ethane is not tested at room temperature, as its boiling point is at  $-88.6\text{ }^{\circ}\text{C}$  [18].

solvent	melting point in $^{\circ}\text{C}$
4-Methyl Pentene	-154
3-Methyl Pentene	-154
1-Pentene	-165
Isopentane	-160
1-Propanol	-126
Pentane	-129
Ethanol	-114

Table 3.2: Melting Point in  $^{\circ}\text{C}$  for tested solvents.

In the experiment, no tested solvent was able to completely solve lipids at  $-140^{\circ}\text{C}$  and within 15 min (Table 3.3). Also streaks of applied lipids did not only stay partially behind, but also new streaks appear on the glass slides. This means that some lipids redistributed on the same glass slide.

Solvent	Result
Pentane	soluble at $-125^{\circ}\text{C}$
4-methyl pentene	insoluble
1:1 volume ratio HFE to 1-Propanol	not mixable, slightly soluble
Liquid ethane	insoluble

(a) EGG-PC

Solvent	Result
1:4 volume ratio 1:2 molar ratio Ethanol to Isopentane	slightly soluble
1:2 volume ratio 1:1 molar ratio 1-Propanol to Isopentane	insoluble
Isopentane	slightly soluble
1-Propanol	at $-130^{\circ}\text{C}$ slightly soluble
Liquid ethane	insoluble

(b) DOPC

Table 3.3: in 3.3a for EGG-PC, no sufficient solubility at  $-140^{\circ}\text{C}$  was found. In 3.3a, DOPC was tested but also no proper solution was found.

Using solvents to remove a sacrificial layer, a high solubility is required. In practice, the sacrificial layer is completely covered by the ice layer except the edges. Therefore area of contact with the solvent is small, slowing the process considerably. Additionally, as the ice layer needs to stay vitrified. The temperature cannot be raised over  $-140^{\circ}\text{C}$  to speed up the process.

The dissolving process of lipids proves to be endothermic. This means that heat is needed to solve lipids, so cold temperature heavily decrease solubility. This effect is observed in the experiment by all solvents to varying degree. It can be assumed that the majority of solvent lipids mixtures are endothermic which is very disadvantageous for finding a potential solvent lipid candidate.

## 4 Separating ice layer mechanically

---

To mechanically separate the ice layer from the sample holder, the adhesion needs to be reduced. Two different approaches are tested: The first approach is using the lipid and Parylene coat for adhesion reduction. The second approach is using PDMS to lower adhesion. In some cases brittleness is used to additionally lower adhesion. To find favorable combinations of mixture ratio and plasma treatment at freezing at specific mixture ratios, tensile tests are conducted at room temperature first. With those results, tensile tests are conducted at cryogenic temperatures of complete samples with a thin ice layer. To further increase likelihood for separation, different factors influencing separation while using the finger are examined.

---

### 4.1 PDMS experiments at room temperature

---

To speed up the process of finding the right balance of PDMS Mixture ratio and plasma curing, experiments are done at room temperature. For this, a pulling machine is used. First the sample is prepared. Then, the sample is clamped to the pulling machine. A Plexiglass stamp is aligned on top of the sample. The relative force and distance is set to zero on the pulling machine. With UV glue, the stamp is glued to the PDMS layer on the sample. After gluing, a couple minutes have to be waited, so no further stress changes are ongoing from the gluing process. After setting the force again to zero, The tensile testing machine is pulling on the sample with constant displacement increase. After detachment, the measurement is stopped. Afterwards, the stamp and the glass piece are analyzed under a microscope. The area of the attached UV glue to the glass piece is determined. With the maximum force and area, the maximum stress is calculated. Each experiment is repeated multiple times.

In section 1.2, papers describing different effects of changing mixture ratio and plasma treatment are presented. In conclusion, a mixture ratio with high curing agent content results in low adhesion without plasma curing. The effect of plasma activation on mixture ratios over 50:1 results in a brittle surface. Still, the effect of plasma activation under 50:1 is unknown. The plasma activation has two effects: first, it increases wettability and therefore adhesion on ice to PDMS. Second, the PDMS changes its structure, which could decrease the strength of the PDMS layer.

In the following, A process is developed to perform tensile testing on a PDMS layer at room temperature. The advantage is a big simplification of the test process, but a certain transferability of the results must be shown. Then the effect of plasma curing on PDMS with mixture ratios of 1:2 base coat to curing agent is investigated and compared to the effect on other PDMS mixture ratios.

Preparation step	PDMS 1:2	PDMS 4:1	PDMS 50:1
Degassing in vacuum	30 min	30 min	1 h
Spin-coating	3000 RPM for 120 min	3000 RPM for 120 min	3500 RPM for 150 min
Baking at 80 °C	24 h	30 min	20 h

Table 4.1: Differences in preparation of different mixture ratios of PDMS. The viscosity is increasing with higher base coat portion which results in longer degassing and spin-coating. Baking time takes longer with higher variation of the mixture ratio from the recommended 10:1 mixture ratio.

#### 4.1.1 Preparation of PDMS samples

All PDMS samples are prepared in a similar way. The preparation starts with weighting out the desired amount of base coat and curing agent. The mixture is stirred intensively. The mixture is placed under a vacuum bell to gas out all air bubbles from stirring. Meanwhile the cover glass used as sample holders are cleaned with ethanol or isopropanol and dried. Afterwards, the PDMS mixture is spin-coated onto the cover glass. Then the coated cover glasses are baked in the oven. The time and other variables needed for each process steps are dependent on the viscosity and the ratio of base to curing agent of the PDMS mixture (Table 4.1).

For shorter baking times at 1:2 mixture ratio, plasma treatment has a slightly different effect. Normally, touching a treated area will neutralize the effect of plasma treatment like hydrophilicity only locally on the touched surface. But here, touching the surface leads to the complete neutralization of plasma treatment when touching. In this work, the effect is undesired.

In the coat spinning setup, each Ø5 mm sample holder is coat-spinned in succession of each other. With each spin-coating taking 2 to 3 minutes, this step can take up to multiple hours. To speed up coat-spinning, rectangular cover glass with 20 mm x 20 mm and 24 mm x 40 mm are used instead. Afterwards the cover glass is split in multiple smaller pieces.

The process is the same described as before for all PDMS mixture ratios, but with some minor adjustments. Before coat spinning, the glass is scratched with a diamond pencil. The scratches in the glass are weak points for breaking out smaller parts. Kapton tape is put over the scratched glass. The glass is put into the coat spinner with the taped side facing down. The PDMS is coat spinned onto the exposed glass side. The baking process is as previously described. After baking, the glass is broken into smaller pieces. This is done by dragging the attached kapton tape over a table edge. Then the glass is fixed to the table with PDMS facing up. The PDMS is covered with Mylar foil to keep the PDMS clean. As the sticky side of the tape is facing up, the Kapton tape ends are additionally taped to the Table. Then smaller sample pieces can be broken off. The pieces are loosened from the tape by forcing a flat pincer between glass and the tape it is attached to.

This method has advantages as well as drawbacks to coat spinning small glass pieces separately. First, time is won by coat spinning, as one big glass can be split into several smaller ones. The sample can stay fixed at the table without risking damaged. The samples can be broken off shortly before the experiment. But manually using a diamond pencil, only irregular and rectangular shapes can be won out of the bigger glass piece. also there is a significant loss of samples. This is by one part by breaking the sample. Some cracks do not follow the scratch, which leads to too small samples. Also in the process of loosening a piece cracks can form, making the piece too small for use.

In the end, both preparation methods are used for different experiments. The Ø5 mm cover glass is used in combination with the finger. The regular pieces are easier set up with the shuttle. The glass pieces broken

out of the rectangular cover glass are used with the pulling machine at room temperature. In this setup, fluctuations in size of the glass pieces are easier to handle and the clamping of the slide is more flexible.

#### 4.1.2 Setup of the pulling machine

To test the tensile strength of different PDMS mixtures and the effect of plasma curing, the tensile testing machine Inspekt table 5 kN manufactured by Hegewald & Peschke is used. On the top part, two load cells are installed (Fig. 4.1a) The upper load cell is rated for 5 kN. the lower load cell is rated for up to 100 N. As the upper load cell is extremely stiff and the forces are  $\ll 100$  N, the upper load cell can be assumed as inflexible. On both the upper and lower part, two clamps are fixed onto the machine. On the bottom clamp a 3D-Printed stage is used for fixing on the sample. (Fig. 4.1b). The stage has four holes with threads for screws. Between the threads, the sample is placed. A brace is fixed with screws onto the sample. A rectangle shape hole in the brace gives access for the UV-glue and the stamp.

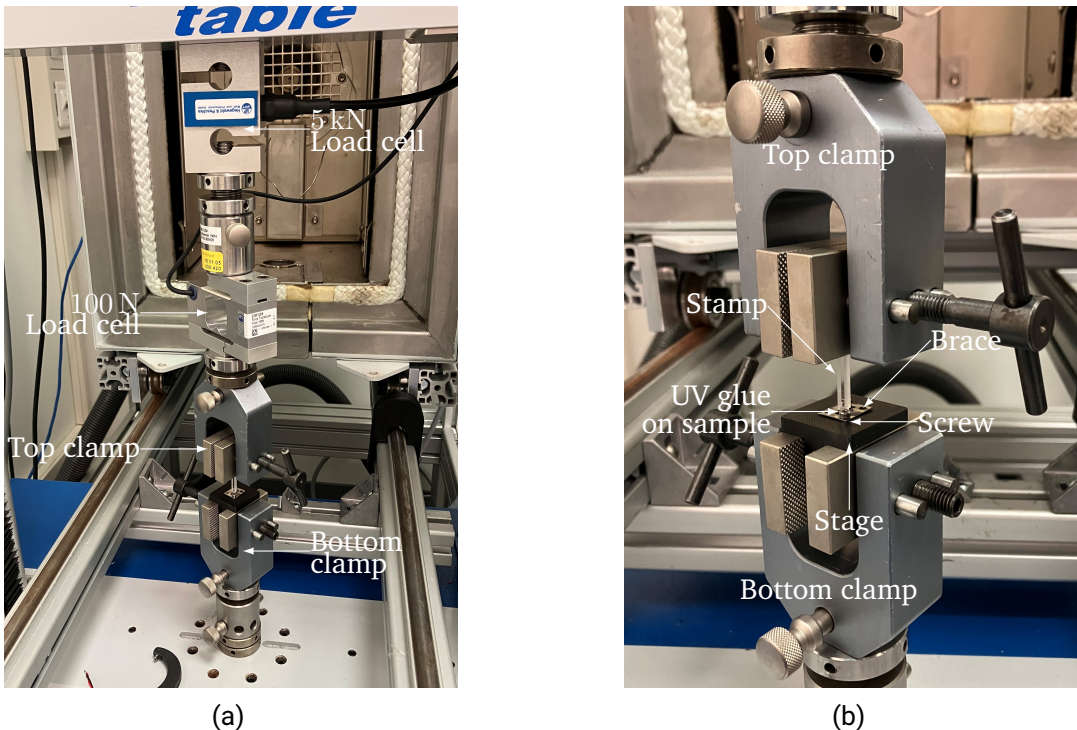


Figure 4.1: Setup for tensile tests of a thin PDMS layer. The Sample is placed on the stage. A brace is screwed over the sample to hold it in place. A stamp is fixed to the top clamp. The UV Glue is applied between stamp and sample and cured with 3 minutes UV Exposure. With the 100 N load cell, the force is measured over distance pulled.

Two different plasma machines are used for plasma activation. In almost all cases, a small plasma machine with a maximum power of 100 W is used. The pressure is around 0.3 mbar for all plasma activated sample holders. Also a bigger plasma machine is used in rare cases. It can deliver a plasma up until 1000 W. Regular air is used for all plasma activation.

#### 4.1.3 Tensile testing of PDMS

The process of a tensile test starts with clamping a new stamp to the top clamp. Then the sample is plasma treated. After treatment, the sample is quickly transported to the pulling machine and fixed to the stage with screws. The stamp is aligned to the clamped down sample. When the stamp and sample is alignment, the UV glue is given onto the stamp. the stamp is lowered on the sample until contact is made with the UV-glue. The UV-glue is cured with UV radiation for 3 min. After gluing, 3 min are waited until forces settle resulting from curing and heat. Then, the tensile testing machine pulls with constant displacement increase of  $0.01 \text{ mm s}^{-1}$  and measures the force over displacement curves. The process is ended manually. The now separated stamp and sample are stored for observation under a microscope. To calculate the maximum tensile stress, the area of the glue on the sample which is still attached to the stamp is measured.

Measuring the area of contact between PDMS and UV-glue is not trivial. Multiple separating layers are visible, which are sometimes hard to distinguish (Fig. 4.2). First the transition between stamp and UV-glue is visible. Then the area between PDMS and UV-glue is on top, which is measured to calculate the tensile stress. Then sometimes there is potentially the ripped of PDMS layer itself. Some reflection in light additionally make finding the correct outline difficult. Still, the relative error when picking the area incorrectly is within 10 %, which is small enough to keep results distinguishable.

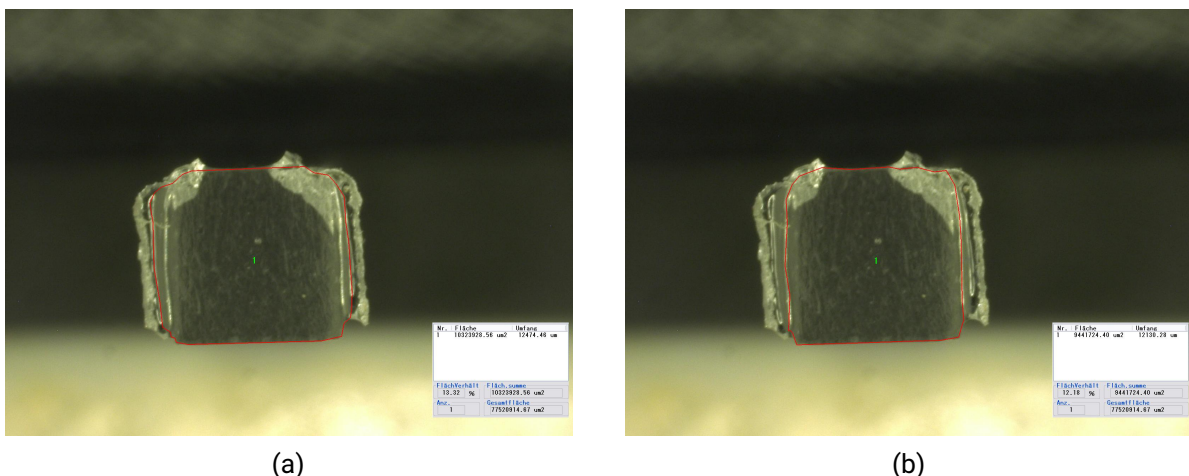


Figure 4.2: Example of two potential outlines of the area and measured area between PDMS and UV-Glue.

As all layers of the contact surface of the stamp, UV-Glue and potentially the ripped of PDMS layer are very close together. The right outline between PDMS and UV-Glue is hard to distinguish. (b) was picked to calculate the tensile stress. This results into an absolute error of 9.34 % if (a) would be the correct area between PDMS and UV-glue. Therefore the error from picking the wrong outline is small enough to keep results distinguishable.

In between experiments, small variations and improvements are done: Two different cross-sections of 2 mm x 3 mm and 3 mm x 3 mm are used in experiments. Since the area is measured by the attached surface to the sample, the effect of the cross-section is taken into account. Also, in first experiments, while waiting of the stress changes to subside, the pulling machine is holding the position. As the UV-glue cools and shrinks after being irradiated, the UV-glue pulls the stamp and the surface more and more together. Before pulling, the machine is set back to zero. An offset exists between before pulling which was set to zero and after pulling when both ends are disconnected. The offset is then corrected in evaluation. To avoid calculating an offset,

the pulling machine sets the distance corresponding to the forces being constant to zero. The offset correction and new method increased the accuracy between pull tests.

To verify the setup, cover glass pieces coated with 4:1 and 1:2 curing agent to base coat weight ratio and uncoated cover glass as control surface are compared. For each, multiple tensile tests are conducted. The force over displacement is recorded and evaluated. An example of raw data is shown in Fig. 4.3. With the area measured of the UV-glue residue on the stamp, The maximum tensile stress is calculated over successful tensile tests with mean and standard deviation.

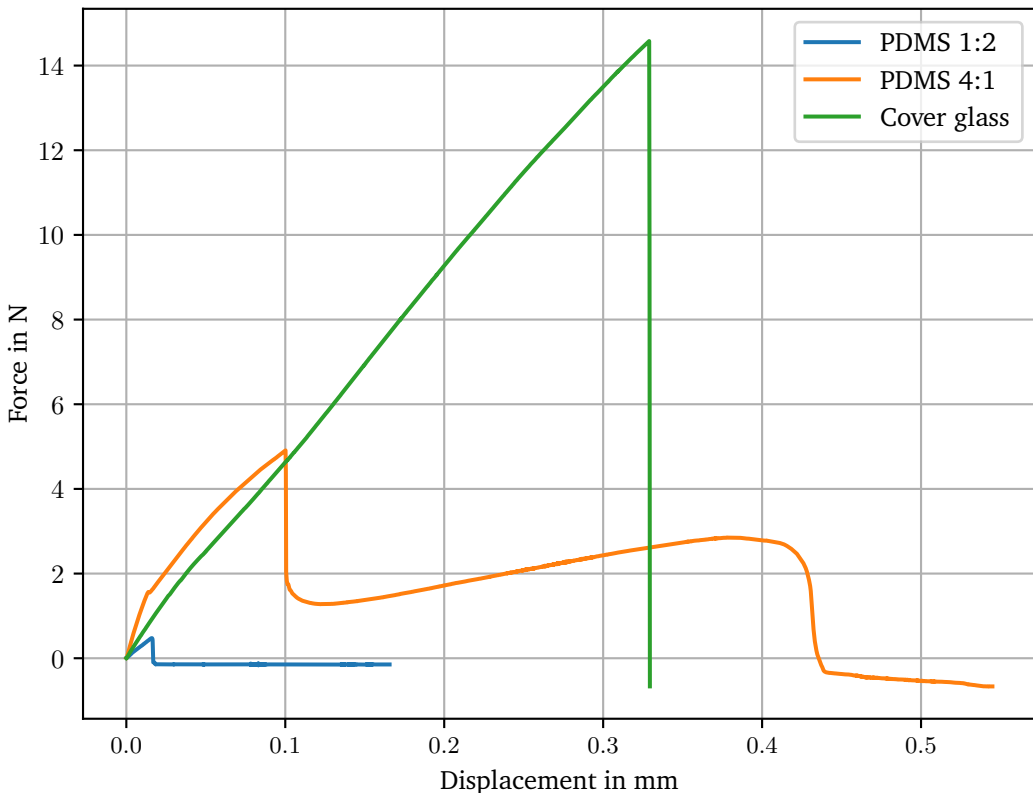


Figure 4.3: Raw data of three different tensile tests with different samples. The different mixture ratios of PDMS are clearly distinguishable. At 4:1, the Force is not dropping to zero after force maximum. A peeling behavior was observed at 4:1. This was also observed in some cases at 1:2 mixture ratio. Most relevant is the maximum force in each test to detach from the sample.

For PDMS coated cover glass, following cases occurring in tensile tests are sorted out. In some cases, the UV glue does not stay connected to the stamp. This suggest that the glue did not adhere well enough to the stamp, potentially falsifying the tensile stress measured. In other cases, the cover glass cracks when testing. These are sorted out for the same reason. Additionally, cases in which the Tensile stress is near or within the uncertainty of the uncoated cover glass are sorted out as well. This can occur when the PDMS coated cover glass piece flips between preparation and clamping down. As some of these cases occur often, randomly and are detected mostly just in evaluation, the repetition rate is low.

The results show 2:1 mixture ratio with  $87.3 \pm 19.9$  kPa has lower adhesion than 1:4 mixture ratio with  $429.1 \pm 5.1$  kPa (Fig. 4.4). Also the cover glass without PDMS takes up a lot more tensile stress up to  $1161.5 \pm 111.5$  kPa. Sometimes the tensile testing machine is able to break the control cover glass. This shows that the UV-glue is stable enough to pull on the PDMS layer.

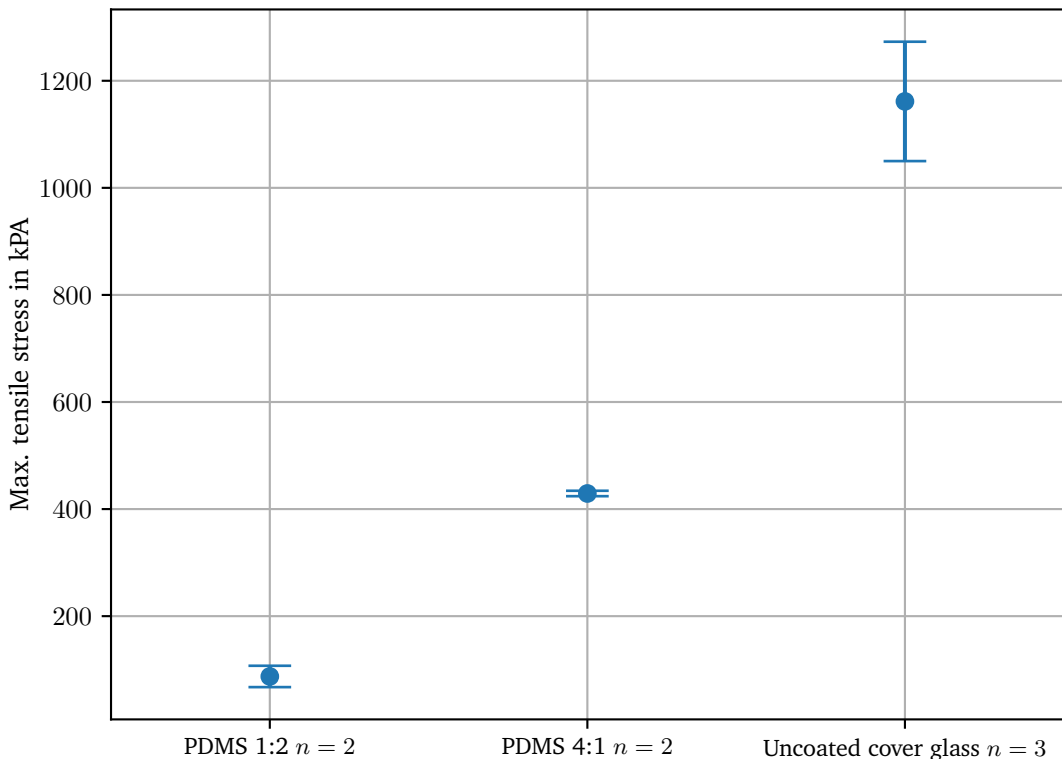


Figure 4.4: Comparison of PDMS with 4:1, 1:2 Base coat to curing Agent mixture ratio by weight coated on a cover glass and cover glass without PDMS as reference. The data points are calculated with the mean and standard deviation of maximum tensile stress. A mixture ratio of 1:2 shows the lowest tensile strength needed to separate the UV-glued stamp from the sample.

In literature, the ice adhesion on PDMS without plasma treatment is 35 kPa. for 2:1 and 5:1 the stress is between 60 to 80 kPa [10]. This is considerably lower than measured values (Fig. 4.4). Therefore, one limitation is that the actual adhesion between ice and PDMS cannot be simulated by this experiment. Still, there is a correlation between values measured and in literature. Additionally, a detachment between other layers than the transition of ice and PDMS counts as successful detachment.

In the next experiment, the effect of plasma curing is investigated. A mixture ratio of 1:2 is examined as this mixture ratio leads to the lowest adhesion to ice and other surfaces. The same setup on the pulling machine is used. Samples with a 2:1 weight ratio PDMS are additionally plasma treated before quickly clamping on the pulling machine. The minimum plasma activation possible with used plasma machine is 25 W at 0.1 min. Below 25 W plasma does not reliably form in the chamber. the maximum tested plasma activation of 2 min by 100 W is additionally done with a bigger plasma machine.

Even with low repetition rates of  $n = 1$  to  $n = 3$ , a clear tendency is visible. With lower and stronger plasma treatment, the tensile stress needed to detach from the PDMS Layer is higher (Fig. 4.5). Over the whole range, The tensile strength of PDMS becomes up to six times higher. Also no visible changes of the surface are observed. This is not expected, as plasma activation on mixture ratios of 50:1 has the opposite effect [12]. This means that this the results are not applicable to other mixture ratios. Also no visible changes to a glass-like state was observed in 2:1 weight ratio mixture. Because the repetition rate is especially low, the exact values should be treated with caution.

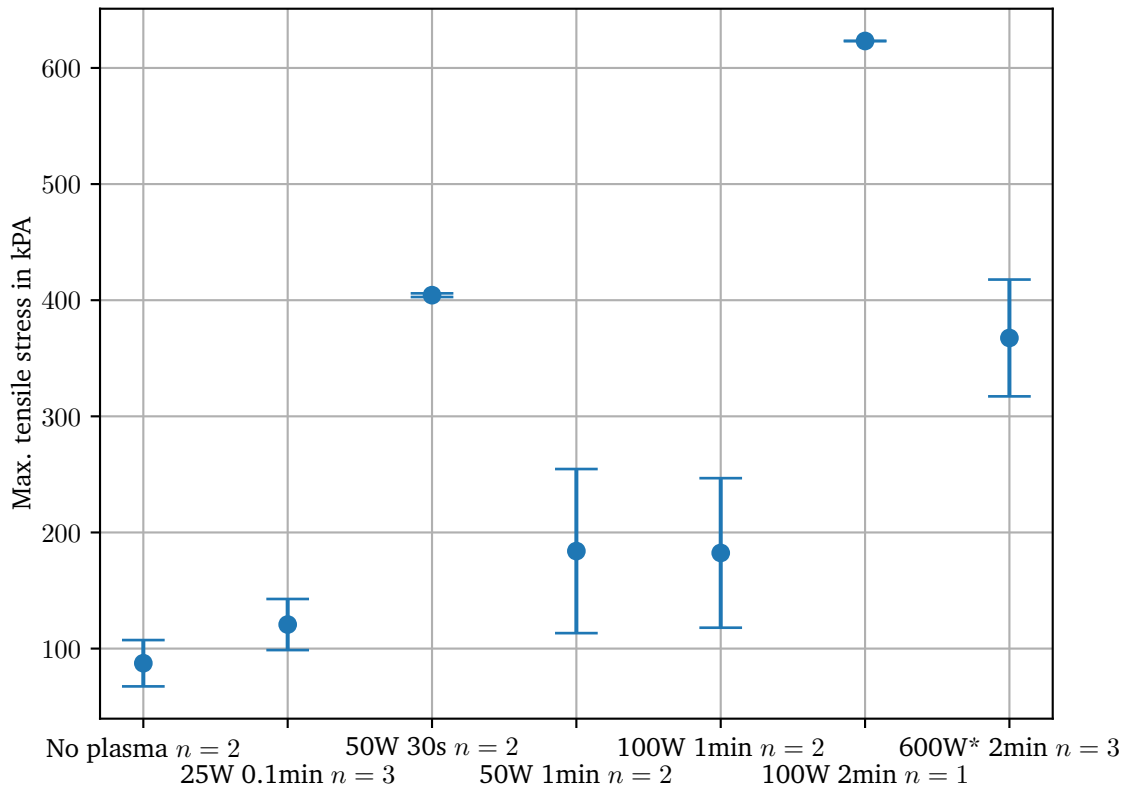


Figure 4.5: Tensile strength of PDMS 2:1 mixture ratio coated cover glass with different plasma activation. Each data point is calculated with mean and standard deviation over  $n$  tensile tests. The last data point with (\*) is plasma activated with a bigger plasma machine. A clear tendency of an increase of tensile stress over intensity of plasma activation is visible.

As PDMS is hydrophobic, plasma activation is needed to freeze a thin layer of ice onto the coated slide. However, super low plasma activation can lead to an insufficient wettability increase. To test the contact angle, PDMS coated slides with mixture ratio 1:2 is plasma activated with 25 W for 0.1 min, 30 W for 0.2 min and 35 W or 0.3 min. 25 W for 0.1 min results in a contact angle around  $45^\circ$ . 30 W for 0.2 min contact angle is around  $15^\circ$ . 35 W with 0.3 min is below  $10^\circ$ . As a control, a PDMS coated cover glass with no treatment and a PDMS coated cover glass with UV treatment of 3 min are compared. The untreated and UV treated PDMS coated glass have both a contact angle of over  $90^\circ$ . Both 30 W for 0.2 min and 35 W with 0.3 min are used in experiments.

#### 4.1.4 Visible changes of 50:1 mixture ratio PDMS with plasma activation

Last, to confirm the effect of plasma activation on 50:1 PDMS, sample holders coated with 50:1 PDMS mixture ratio is compared with 25 W power at 3 min, 100 W power at 3 min and 100 W power at 10 min. With increasing power and time, cracks start to form. This observation aligns with the results in [12].

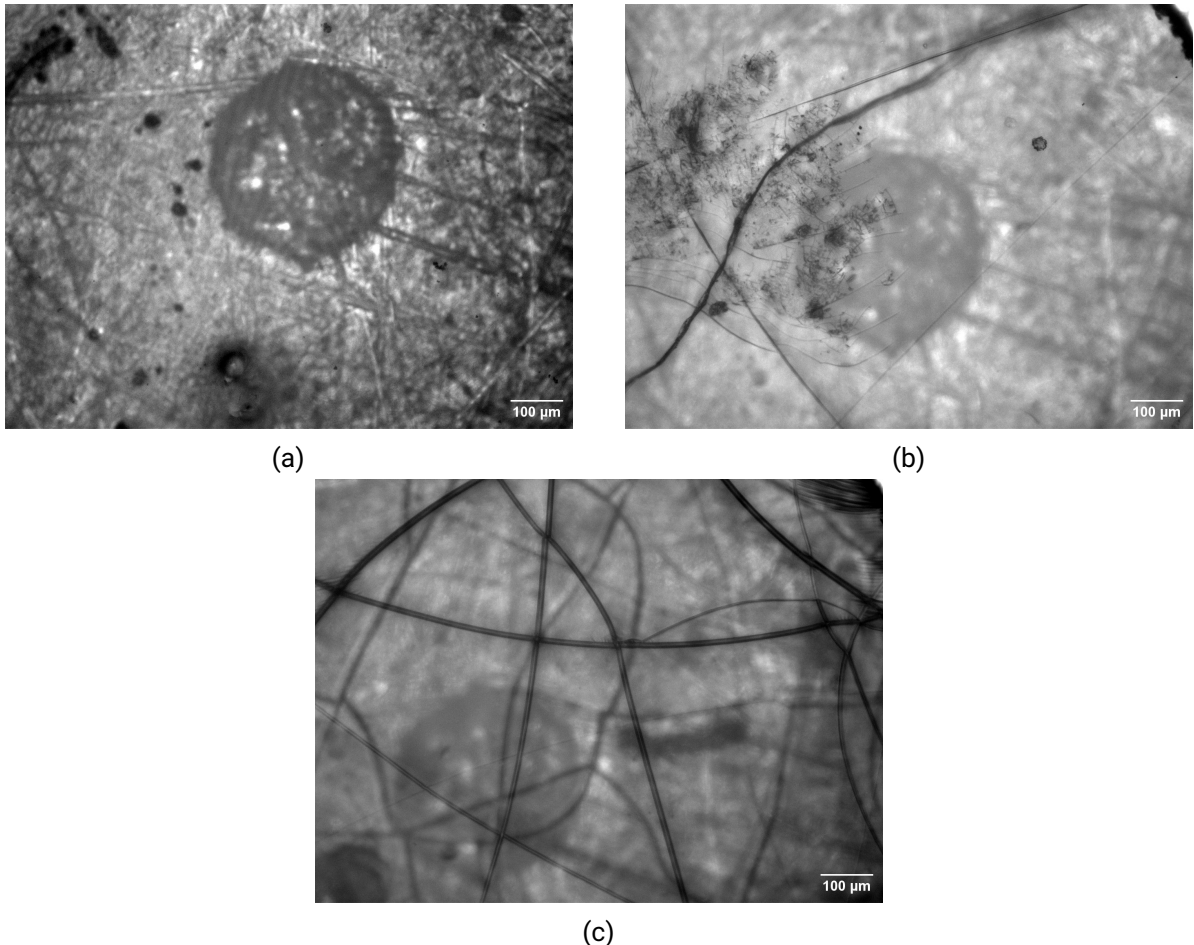


Figure 4.6: Comparison of different plasma activation on PDMS with 50:1 mixture ratio. In (a), 25 W power at 3 min leads to no crack formation. The PDMS is transparent showing the central mark of the copper shuttle. In (b), 100 W power at 3 min leads to cracks. Increasing the duration to 10 min at 100 W power increases the cracks. The cracks indicate increased brittleness of the surface.

## 4.2 Experiments at cryogenic temperature

To actually try to separate an ice layer from sample holder, experiments are done to archive separation. The aim is to test the reduction of adhesion of the engineered layer. With enough reduction of adhesion and enough force applied, the ice layer should separate.

Separation of the ice layer is tested on parylene and lipid coated sample holder as well as PDMS-coated sample holders with different mixture ratio and plasma curing. Different variables of the finger are examined

to increase tensile strength applied and reliability.

For all experiments, Ø5 mm cover glass is used as sample holder. These cover glass used as sample holders have a higher thermal conductivity resulting out of different composition and increased thickness than sapphire sample holders typically used for cryo-LM. Therefore no or only partial vitrification of the ice layer is reached. Therefore a slight reduction of ice adhesion is expected by using non vitrified ice. Also, the costs of using cover glasses is very low. Therefore using cover glass holders is sufficient for first experiments and experiments with vitrification can be followed up later.

Two different setups are used. First, the setup with finger and bath is used. Second, for additional data, a modified version of the setup with the pulling machine is used. This allows the measurement of the actual tensile strength on the sample.

To try out the separating with the finger in a repeatable manner, a core process is established. The sample is plunge-frozen with distilled water containing fluoresceine. The copper shuttle is placed in the harbor. With HFE, the sample is placed in the middle of the shuttle. The HFE helps the sample to stay in place before fixation. The "window" brace is placed on top and screwed down. The now prepared shuttle is transported quickly to the microscope for pre-imaging. When the transfer is not possible within seconds, the shuttle is placed in a portable container with liquid nitrogen. After microscopy, the sample is placed into the bath under the cooled finger. The HFE is applied and the finger is lowered in "unglue" mode. When the HFE touches the sample, the temperature is cooled with "glue" mode. When the final temperature is reached, the finger is pulled up. To confirm detachment of the ice layer, the shuttle is transported to the microscope for post-imaging. The images are compared for changes of the fluorescent ice layer.

#### 4.2.1 Preparation of samples

The sample preparation are based on the steps used in cryo-LM. Plunge-freezing is used to freeze the ice layer to the sample holder. This process is done manually and with a plunge-freezer. For both, the steps are the same. Generally, plunge-freezing manually should give similar results to a plunge-freezer. More flexibility and a faster process is reached by freezing manually but higher consistency is reached by a plunge-freezer.

To successfully plunge-freeze a sample, following steps are taken: First, the slide is held by tweezers. Then a 2 mL water drop containing fluoresceine is pipetted onto the hydrophilic sample holder. The fluoresceine content varies between 10 mg/50 mL to 10 mg/5 L distilled water based on the microscope setup. The water droplet is blotted with filter paper, creating a thin film of water which evaporates quickly. The tweezers holding the slide is shot in cold liquid under  $-140^{\circ}\text{C}$ , typically liquid ethane. The rapid temperature drop freezes the water into a thin layer of ice.

To create vitrified ice, The liquid which is used to freeze the sample should not possess the Leidenfrost effect, which prevents instant contact of the sample with the cold liquid. As liquid nitrogen is possessing the Leidenfrost effect, other coolants like liquid ethane are used. In this master thesis, samples frozen manually are not given into liquid ethane, as additional preparation must be done with higher safety risk without improving sample quality, as the sample holders used greatly inhibit formation of vitrified ice.

For storing samples after plunge freezing over prolonged time, boxes with space for three Ø5 mm samples are designed (Fig. 4.7). These are 3D Printed, modified version of grid boxes. a grid box cap is screwed on top with a specialized tool. Inside a bath, grid boxes and the compatible 3D-printed container fit into the indents. The cap is screwed next to the container, clamping it down to the work surface. Also the container are interoperable with tools used for grid boxes. This allows long term storage of samples with 5 mm diameter.

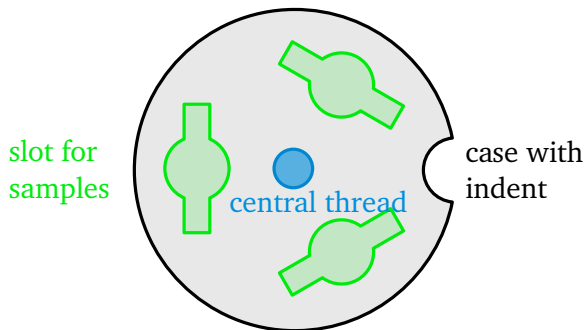


Figure 4.7: Small 3D-printed transport box for three samples. A cap is screwed onto the central thread. These boxes fit into storage units. The design is based on a commonly used storing system.

#### 4.2.2 Inverted microscope

To take detailed pictures of the sample, an inverted microscope is modified for cryo- microscopy (Fig. 4.8). The microscope is able to image fluorescence light. For this, filters are swapped between real light images and fluorescence images. A 2-fold and later 5-fold objective is used for imaging. A cryo-stage is added to cool the sample to cryogenic temperatures. The box is designed for a non-inverted microscope. One goal of this setup is to test the applicability of cryo-LM on inverted microscopes and which modification should be made to improve the setup.

The cryo-stage with a copper heat sink is fixed to the bottom of the stage (Fig. 4.9). The box is supplied with cold nitrogen gas to cool the heat sink. A haven is fixed to the heat sink and placed over the objective. The haven is temperature controlled to  $-140^{\circ}\text{C}$ . The "glasses" component keeps the light path between haven and objective clear from ice and fog. It contains two thin and parallel glass panes. Warm nitrogen gas is routed between the glass panes and out between the lower glass pane and objective. Under the glasses, a shuttle containing the sample is placed in the harbor.

The shuttle allows easy transportation and access to the sample. The sample is clamped down by the "window" brace (Fig. 4.10). The window brace is fixed with two screws to the shuttle, holding the sample in place. A center hole in the window gives access to the top side of the sample for microscopy and finger. In the copper shuttle a thread is placed. With a long threaded metal rod the sample is transported between assemblies.

In general, The inverted cryo microscope was successfully used throughout this master thesis. Still, many improvements should be made to increase usability and accessibility of the inverted microscope.

To take pictures, a two-fold and 5-fold objective is used. The 5-fold objective fits between the microscope and glasses assembly without a significant gap. However, to fit the 2-fold objective the glasses assembly needs to be redesigned thinner. With the increased gap between objective and glasses assembly, more ambient light is creating noise. This decreased the visibility of fluorescence on samples. With the increased field of view with the 2-fold objective, total reflection of the two glass panes in the glasses assembly is inducing strong noise in the pictures. Also the access hole to the harbor is a bit too small.

To reduce noise and increase the harbor access, the glasses assembly is fixed tilted to the box by adding spacers. In future, the glasses assembly needs to be redesigned to hold tilted glass panes. When using multiple objective with different magnifications, The sample must be additionally shielded from ambient light to increase visibility.

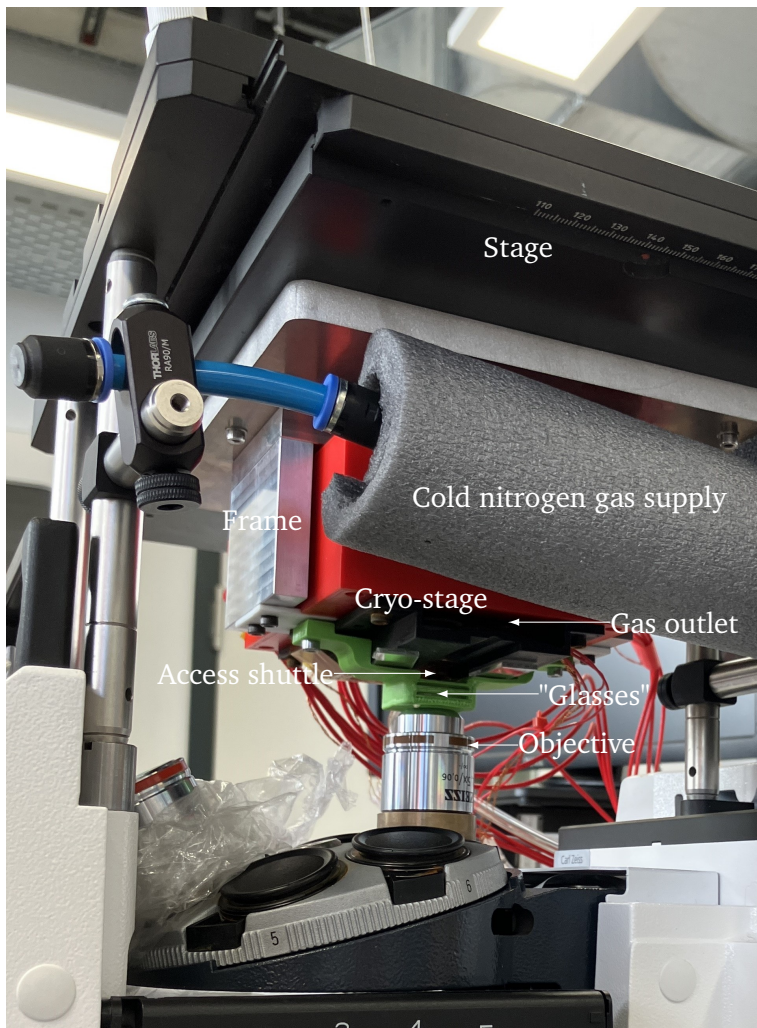


Figure 4.8: Modified inverted microscope for cryo-LM. A cryo-stage is added to let the sample stay cool at cryogenic temperatures (fig. 4.9).

Besides the "glasses", the exhausted gas decreases accessibility of the harbor. The exhausted cold gas over the harbor results in fog and locally reduces oxygen. As the fog falls down over distance, the access point is only visible in certain angles. The big stage and cooled box on top additionally reduce visibility to the access point. In future, the exhaust should be pointed away from important access points.

Ice frozen to the assembly can also damage the microscope. Especially when the setup warms back up to room temperature, the ice melts and water drops onto important parts. Therefore, the objectives should be designed water proof. Gaps should be closed as much as possible to avoid water entering the inside of the microscope.

#### 4.2.3 Baths

In the beginning a smaller bath is used (Fig. 4.11). The small bath contains an elevated work surface. Embedded in the work surface are indents which fit container holder. Three elevated baths are installed on the elevated floor. They are temperature controlled by a Pt-1000 sensor and heater for containing other

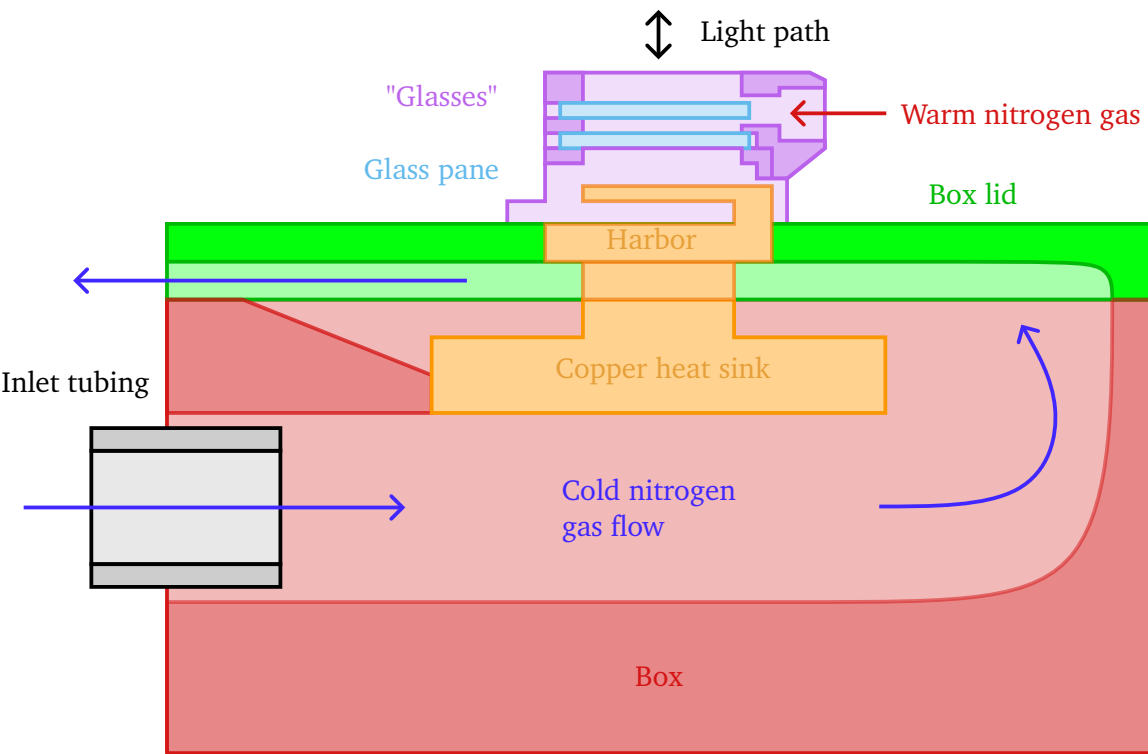


Figure 4.9: Cross-section of the added cryo-stage to keep the shuttle and sample cool. The harbor is fixed on the copper heat sink. The heat sink is cooled by cold nitrogen gas flowing trough the box keeping the heat sink cool. Below the box lid, the cold nitrogen gas is exhausted into the environment. The glasses assembly keeps the light path clear.

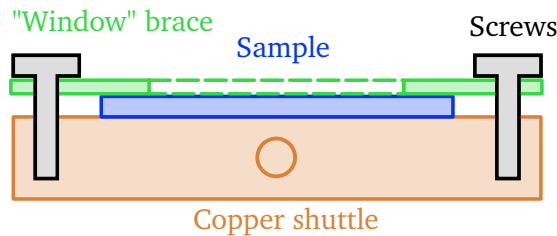


Figure 4.10: Shuttle for transporting a sample between bath and microscope. The window is clamped down by screws to the copper shuttle, holding the sample in place. the center hole in the window gives access for microscopy and finger.

liquids or tools at different temperatures. Also a Haven for a shuttle system is installed. The small baths and the haven are separated from the elevated floor by an insulating layer. The bath is filled with liquid nitrogen covering the work surface. The whole bath is insulated by Nitrogen gas flowing inside the 3D-printed shell around the bath. The warm nitrogen gas is expelled from the brim, flowing from the outer edge radially to the middle rotation axis.

The usage of the small bath in combination with the finger has limitations: First, the space in the bath is small. The finger can be moved along the track, but the space left still limits work with pincers. Additionally, the smaller temperature controlled baths are not needed when using the finger, therefore taking up much needed space. Also the shuttle needs to be tilted in a specific angle to dock and undock the shuttle. The work flow

also allows only one shuttle at once, limiting throughput. Liquid nitrogen needs to be refilled often since the bath can only hold a small volume.

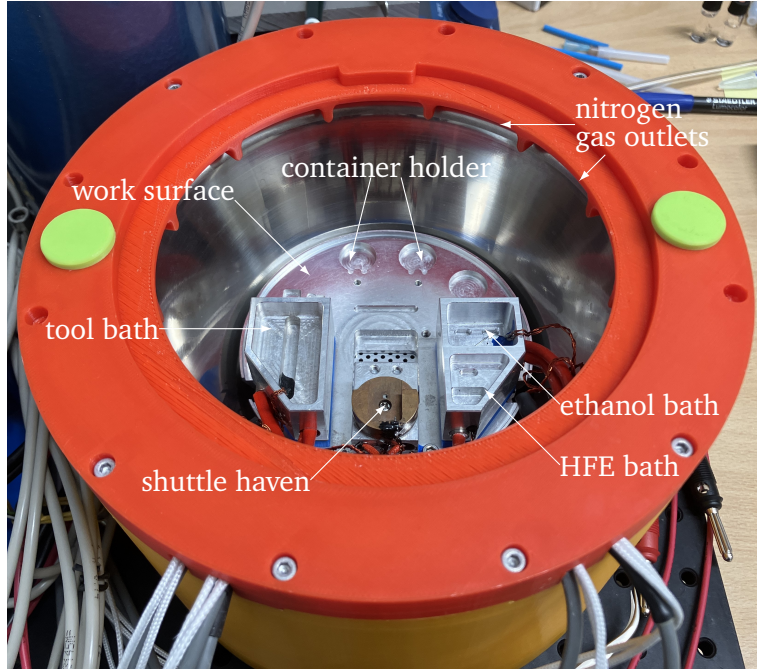


Figure 4.11: Small bath used for sample preparation. This bath is used in combination of the finger. A major drawback of use with the finger is the lack of space inside the bath. To solve this issue, a bigger bath is constructed.

During this master thesis, a second bigger bath is build (Fig. 4.12). In general, the structure is similar. It also uses an elevated floor as a work surface. The work surface is fabricated out of two plates screwed together and fixed to the brim with 3D-Printed hooks. Indents are formed by holes in the upper plate. No baths are installed, but the space is reserved for later additions. Two harbors are mountable for parallel work on two separate shuttles. The harbors are screwed on an aluminum block with sensor and heater for temperature regulation. Between the aluminum block and the work surface, a 3D-printed insulating spacer is placed. Also both harbors can be mounted either flat or in an angle, depending of the 3D printed spacer. The bath is insulated with Styrofoam and a rim with holes for warm nitrogen gas is placed on top. The holes are places along the inside of the long perimeter.

In practice, the bigger bath is more pleasant to work with. The additional access speeds up the preparation progress. Less attention must be paid to keep the nitrogen level over the working surface. The funnel system is less used as the funnel does not stay in the desired place. In the end, one shuttle is used. The camera angle is worse than in the small bath. Originally, The frame for exhausting warm nitrogen gas is placed directly on the bath rim. The finger was not completely submerged under the barrier, leading to light ice formation. The exhaust frame is elevated by 2 cm with Styrofoam.

#### 4.2.4 Finger

The finger is made of two main parts: The first part is a metal rod with a flat tip (Fig. 4.13). The rod is cooled with cold nitrogen gas. Near the tip, the rod is temperature controlled with a Pt-1000 used as a temperature

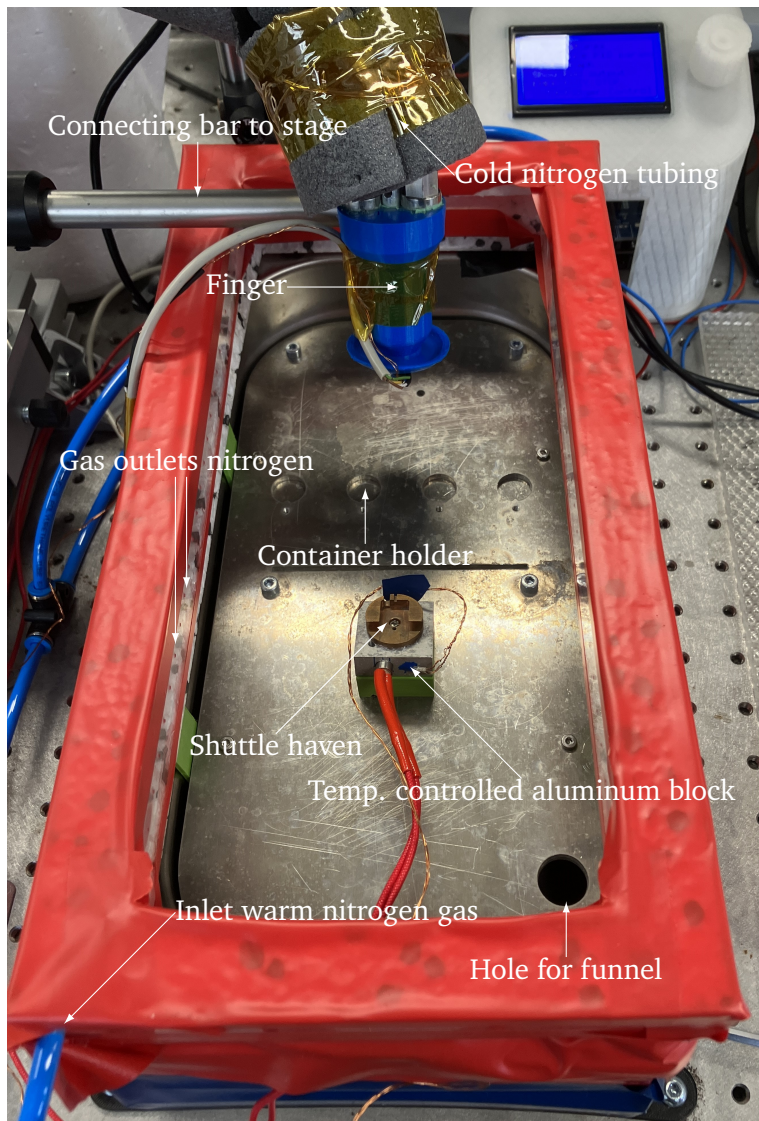


Figure 4.12: Big bath with finger assembly. Inside the bath samples are prepared. When applying forces with the finger, the sample fixed on a shuttle is held in place by the harbor.

sensor and a heater. The second part is a 3D printed structure, containing the outer layer and routing of the cold gaseous nitrogen. Inside the 3D printed structure, the cold nitrogen gas is directed from the inlet downwards around the metal rod in an inner mantle for cooling. Then, the cold gas is redirected upwards flowing through an outer mantle for additional cooling. Afterwards, the gas exits through the output.

The cold nitrogen gas is supplied by a liquid nitrogen tank. Heaters placed inside the tank evaporate the liquid nitrogen. The evaporated gas leaving the tank is routed by 6 mm pneumatic tubing to the finger inlet. On the inlet and outlet of the finger, Festo pneumatic tube connectors are mounted to allow easy dis- and re-connection of 6 mm tubes. Cold nitrogen gas which passed through the finger are exhausted by outlet tubing into the atmosphere.

The finger is mounted on a three stages. These stages allow fine adjustment of the finger position in X,Y and Z axis (Fig. 4.14). Also, when the finger is attached to a surface, force can be applied by moving the stages in

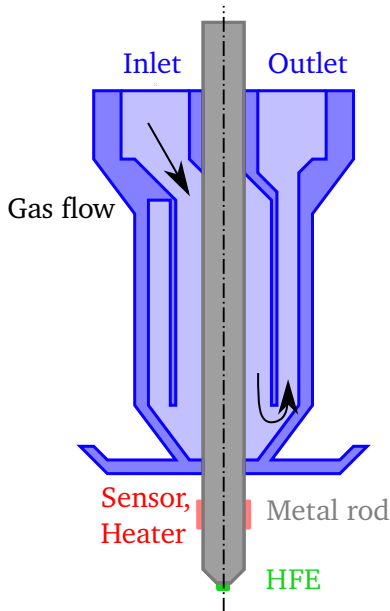


Figure 4.13: A cross-section of the finger assembly. The metal rod is cooled with cold nitrogen gas. The gas is routed from the inlet around the metal bar onto an outer layer to the outlet. The metal rod is temperature controlled by a Pt-1000 temperature sensor and a heater. With HFE 7200 applied to the tip, the finger can attach to a surface at cryogenic temperatures and apply force.

either direction. Additionally these stages are mounted on a track. The track allows more movement along one axis to make assemblies below the finger reachable. Whenever the finger is used, the assembly is clamped down to the track to prevent additional movement.

On the tip of the finger, Ethoxynonafluorobutane, also called Hydrofluorether 7200 (HFE) is used throughout all experiments. HFE is used as cooling agent [19] as well as an cryoimmersion fluid [20]. HFE has temperature dependent characteristics. At freezing point, HFE reaches a viscous state before reaching a firm solid state. This temperature dependency allows to first apply the HFE at higher temperatures with low viscosity and pull on the sample at lower temperatures with high viscosity.

The temperature regulation of the finger has three modes: First the "unglue" mode which regulates the Temperature to  $-140^{\circ}\text{C}$ . HFE has a low viscosity, which allows the application of HFE. Also separating the finger off the sample without transferring force is possible. Second, in "glue" mode the shuttle and the finger are cooled to  $-160^{\circ}\text{C}$ . HFE hardens and force can be applied to detach the ice layer. Third, "thaw" cleans the finger by heating the tip to  $20^{\circ}\text{C}$ , evaporating everything stuck on the finger.

#### 4.2.5 Setup pulling machine for cryogenic tests

To allow tests at cryogenic temperatures with the pulling machine, the setup is modified to allow fitting a bath and the finger to the pulling machine (Fig. 4.15). The big bath is used with a flat harbor. An outer frame is used and modified to hold the bath. The bottom clamp is removed and the bath is fixed over the bottom attachment. The top part is used with the same load cells, but with a bigger clamp. The "finger" 3D printed shell modified with a flat outer profile for clamping and clamped onto the top.  $90^{\circ}$  Festo tubing is used to connect the cold nitrogen gas supply. A power source and a temperature regulator is again used.

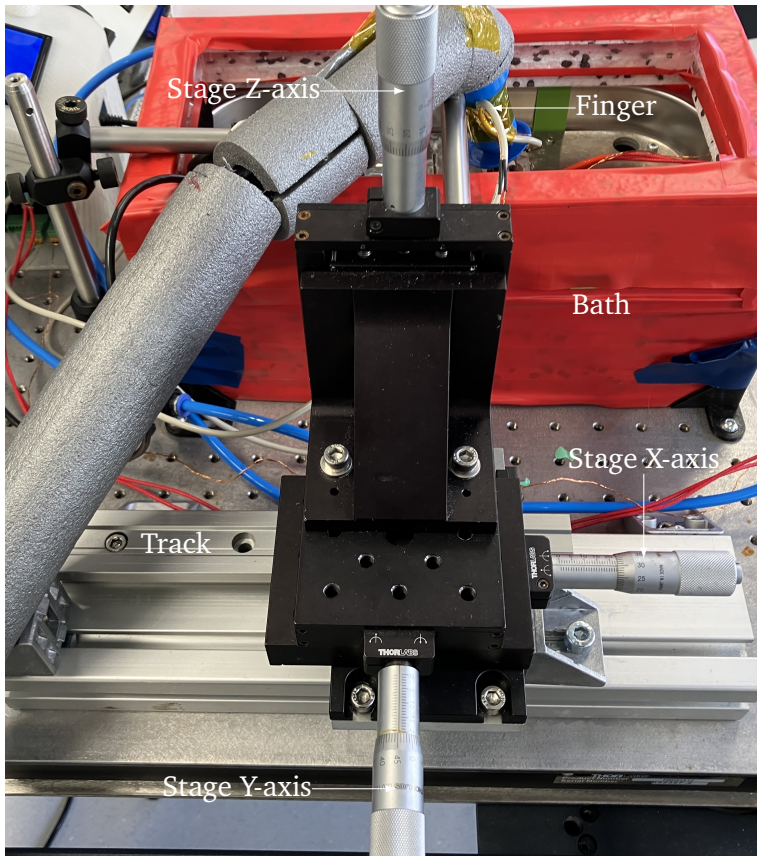


Figure 4.14: Stages to precisely manipulate the finger tip in X, Y and Z direction. When the finger is not in use, it is moved along the track to allow access to assemblies below.

Compared to the finger setup with stages, the finger only moves up and down. The Alignment is done by moving the bath by loosening the screws on the frame. Also new window parts with a bigger central hold for easier alignment are water-jet cut.

As the tensile testing machine is set up in a separate room, the samples are prepared in the laboratory next to the microscope. The small bath is used for sample preparation. The process is the same as all detachment trials with the finger.

This setup has a lot of limitation. Aligning the finger is very difficult, as the screws are hard to reach in cold temperature. When cooling, the previous alignment is lost as the coldness distort the setup. Also little movement at the finger has maximum effect on the sample and alignment. touching the tubes can loosen the sample and/or the setup needs to be new aligned. Even a bigger window is not enough. Errors in alignment and therefore gluing to the border of the window and loosening through movement are the two biggest error sources in this setup. So the old setup is used in further experiments to eliminate big error sources.

#### 4.2.6 Factors observed influencing detachment with finger

To increase the reliability and force applied through the finger, different variables are found and the influence examined. The volume of HFE on the finger tip can improve both force and repeatability. higher temperatures

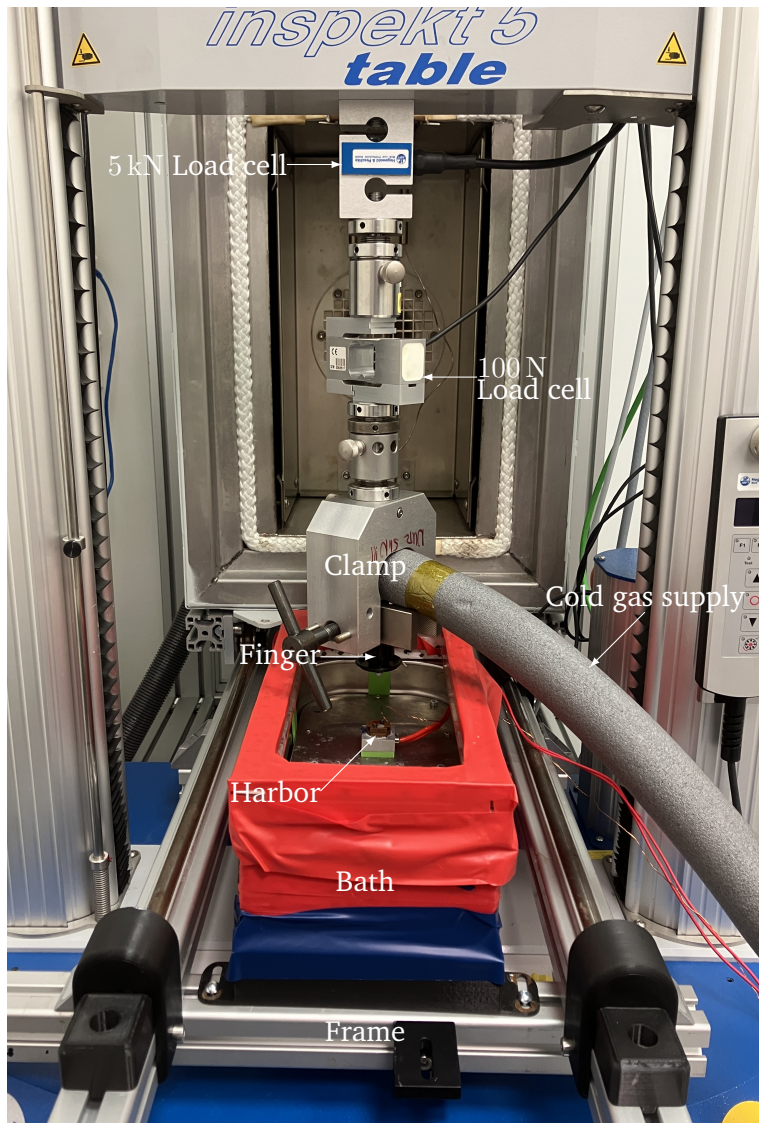


Figure 4.15: Setup finger and bath on tensile testing machine. A frame is added to support the bath to allow cooling. The finger is clamped to the top and is supplied by cold nitrogen gas.

can increase the tensile strength of HFE. The direction of force can decrease the force needed for detachment. Right positioning is also important, especially finding the right gap. Additionally, other factors with less significance are also found.

### **Volume of Hydrofluorether on finger**

Using the correct amount of HFE on the finger tip is important for higher repeatability. Too little HFE will not bind to the finger and sample. Using too much HFE results either in a thicker layer, or the HFE flows between window and sample. as the cohesion of the HFE is considerably lower than the sample and the finger, a thick layer is prone to breaking before the ice layer. HFE under the window clamp will redirect a part of the force, making the sample more stable. This makes detaching also harder.

At the start, the HFE was applied with a pincer. The HFE is given in a cold bath at  $-140^{\circ}\text{C}$ . HFE gets more viscous at colder temperatures and is evaporating much slower. The thickened HFE is now scooped with pincers onto the tip of the finger.

The HFE is dosaged with a pipette onto the tip of the "finger". While pipetting, around  $4\ \mu\text{L}$  of HFE is evaporating. Based on this knowledge, dosaging  $4.10\ \mu\text{L}$ ,  $4.30\ \mu\text{L}$  and  $4.50\ \mu\text{L}$  is compared and a video is taken for later comparison.

The videos show that pipetting HFE is not reliable. The visible HFE volume on the tip does not correlate with the dosaged volume. One reason is a difference in the volume of HFE evaporating while applying. Also some HFE may be placed on the side of the tip. When using the finger, only the HFE on the flat tip is effective.

Another way to determine the Volume of HFE on the finger is by analyzing pictures of the finger with HFE. The volume is calculated with the contact angle on the finger and the area covered in HFE. With the knowledge if the HFE spreads too much or not being attached properly to the sample, a range can be given where success is more likely. Still, other factors like temperature or the gap between sample and finger can influence the result.

Still, a visual estimate for the correct glue dosage is made by calculating the drop volume out of camera images. Two exemplary Pictures of an upper and lower limit of glue dosages is picked (Fig. 4.16). Then the volume is calculated with a formula for the volume of a spherical section. All needed components are calculated out of the estimated contact angle of the glue  $\approx 45^{\circ}$  and the tip diameter of  $1.68\ \text{mm}$ . For the lower range a reduction of the diameter by a factor of  $\frac{2}{3}$  is assumed as the drop is not covering the whole tip. The resulting volume range of the HFE is  $0.11\ \mu\text{L} \gtrsim V \gtrsim 0.38\ \mu\text{L}$ .



(a) Lower limit HFE volume



(b) Upper limit HFE volume

Figure 4.16: Visual representation of the range of dosages which are the most reliable. less HFE than the lower limit is more likely to not attach to the sample properly. more HFE than the upper limit will spread under the window brace or results in a thick HFE layer with less tensile strength.

## Temperature

HFE has a freezing point of  $-138^{\circ}\text{C}$ . Below the freezing point, HFE gets increasingly viscous first. At a certain point, the HFE gets brittle and cracks start to form by decreasing temperature. Between the freezing point and the point of cracking, HFE is usable similar to glue. With a temperature near the freezing point, HFE can spread over the surface. At lower temperatures, HFE gets hard enough to hold the finger to the upper ice layer.

As HFE is getting harder with temperature, lower temperatures in the "glue" state could allow higher forces on the ice layer. Still, the point where HFE starts to crack will decrease the tensile strength. To test this hypothesis, HFE is examined at temperatures below the freezing point.

To test the viscosity and crack formation of HFE below freezing temperature, HFE is given into a small temperature controlled bath. The temperature is regulated from  $-150^{\circ}\text{C}$  to  $-170^{\circ}\text{C}$  in  $5^{\circ}\text{C}$  steps. After reaching  $-170^{\circ}\text{C}$ , the temperature is regulated back to  $-150^{\circ}\text{C}$  in  $5^{\circ}\text{C}$  steps. Changes in HFE when cooling and heating up are observed. A needle is put in the HFE to induce forces and subjectively test the viscosity of HFE at all temperatures.

At  $-150^{\circ}\text{C}$  to  $-155^{\circ}\text{C}$ , the HFE is still only lightly viscous. The needle is not held up by the HFE's viscosity. At  $-160^{\circ}\text{C}$  to  $-165^{\circ}\text{C}$  the HFE is viscous enough so that the needle is able to stand free in HFE. The needle can be pulled out without leaving a gap. Also with more force, the needle can penetrate the HFE. Also no cracks formed so far. At  $-170^{\circ}\text{C}$ , HFE hardens further. The HFE is still viscous. Wiggling the needle in the HFE can result into cracks. Then the needle can be easily pulled out. Under  $-170^{\circ}\text{C}$ , cracks form without inducing forces in the HFE.

Heating the cracked HFE up leads to the cracks eventually disappearing. At  $-165^{\circ}\text{C}$ , first cracks disappear, but many remain. The cracks left are still lowering the mechanical stability of the HFE. Heating up to  $-160^{\circ}\text{C}$  results in further but not complete closing of cracks. A temperature of  $-150^{\circ}\text{C}$  is needed for all cracks disappearing.

In conclusion, maximum load can be applied at  $-165^{\circ}\text{C}$ . Higher temperatures result in lower viscosity, which lowers the maximum stress before HFE breaks. At  $-170^{\circ}\text{C}$ , cracks will form, lowering the maximum stress. To test if desired temperatures are achieved with the finger setup, tensile tests are done with decreased "glue" temperature.

The finger setup is used as described, except the temperatures of the finger is lowered to  $-165^{\circ}\text{C}$  and  $-170^{\circ}\text{C}$  in the "glue" state. With attention to proper insulation and no leakages of cold nitrogen gas,  $-165^{\circ}\text{C}$  is quickly reached and is held stable by temperature regulation over a time span of minutes. Still, the setup is not very reliable as new leaks can form and changing of tanks/tubings can lead to new leaks. These leaks are spotted only when the finger is already cooled. To fix leaks, the setup needs to warm up.  $-170^{\circ}\text{C}$  can sometimes be reached with the finger, but holding the temperature stable is not possible.

When cooling down to the desired temperature with the "glue" state, liquid nitrogen is refilled to increase cooling. When refilling and cooling at the same time, rapid cooling happens when liquid nitrogen touches the shuttle directly at refilling. With this, the Temperature can shortly drop below  $-170^{\circ}\text{C}$ . This induces cracks in HFE, lowering the tensile strength. If this happens, the Sample and finger can be heated up to the "unglue" state at  $-140^{\circ}\text{C}$  and the cracks disappear. Then cooling can start again.

In conclusion, the finger "glue" temperature is most effective at  $-165^{\circ}\text{C}$ . Still, the reliability suffers through leaks, longer tubing and improper insulation. For better repetition, a temperature of  $-160^{\circ}\text{C}$  is also used in experiments.

## Applied Tensile force to HFE

Forces applied to the sample by the finger are unknown. To measure the force transferred to a sample, the setup of the tensile testing machine in combination of the finger is used.

Over all pulls, the HFE can transfer a maximum force of  $1.30 \pm 0.49$  N. The exact size of the area which experienced the force is unknown. Additionally, the force distribution is uneven (e.g. like Fig. 4.17c). A worst case and a best case which are easily calculated can be determined. In the best case, all force is evenly distributed under the area of the finger (Fig. 4.17a). With this assumption, the area is equal to the flat finger tip. The worst case is an even distribution over the whole exposed ice surface (Fig. 4.17b). The surface is restricted by the window center hole. So the inner diameter of the window is the worst case area. In reality, the force distribution is somewhere in between (Table 4.2).

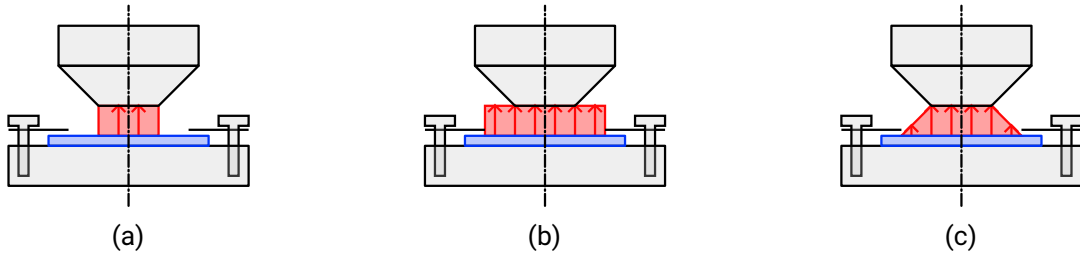


Figure 4.17: Different worst- and best case examples of force distribution on sample. In best case, the force is concentrated on the small area around the finger tip (a). In worst case, the force is evenly spread over the whole sample (b). In reality, the force distribution is between shown extremes. One example of a realistic force distribution is shown in (c).

Area used	Area size	Max. tensile stress
Finger	$2.217 \text{ mm}^2$	$585.4 \pm 219.4 \text{ kPa}$
Small window center hole	$4.91 \text{ mm}^2$	$264.3 \pm 99.1 \text{ kPa}$
Big window center hole	$12.56 \text{ mm}^2$	$103.3 \pm 38.7 \text{ kPa}$

Table 4.2: Tensile stress and size of area used to calculate the tensile strength of the finger setup. In worst case, the force is distributed over the whole "window" size (Fig. 4.17b). In best case, the force is only distributed on the "finger" tip (Fig. 4.17a). The real value is between those extremes.

In contrast, the adhesion on 1:2 mixture ratio without plasma activation has an ice adhesion strength of 35 kPa. 50:1 mixture ratio even without plasma activation has 60 kPa ice adhesion strength [10]. This suggest that detachment should be generally possible. However, other factors like stability of the ice layer and plasma activation will change the actual needed tensile strength.

### Direction of force

The direction of force can increase the likelihood of a successful separation. For example, to remove a suction cup from a flat surface, using tensile force by pulling up will take a higher force than by sliding the suction off the surface with shear forces. The same could apply to the sample. To test this hypothesis, tests are done by applying force in different directions.

In research, PDMS shows less adhesion forces on ice if tensile stress is applied [10]. Still, HFE stability to shear stress is not known. Additionally, the sample is clamped down to the top. This does not allow the ice surface to slide off without breaking.

In most experiments, the shuttle is tilted around 15 degrees for easier access to the shuttle. The finger is also tilted so the tip surface is parallel to the sample. To apply force, the finger is pulled by stages in either X, Y, or

Z direction. For each direction, the resulting stress can be split into tensile and shear stress. In Z direction, mostly tensile stress is applied (Fig. 4.18 (a)). In X direction, mostly shear stress is applied (Fig. 4.18 (b)). In Y direction, only shear stress is applied. But detached pieces moving in Y direction will collide with the clamped down part of the ice layer. This could shatter the ice layer and take more force. Additionally, the sample is clamped down only by friction, strong forces in Y direction could slide the sample inside the shuttle. For this reason, only X and Z direction are tested.

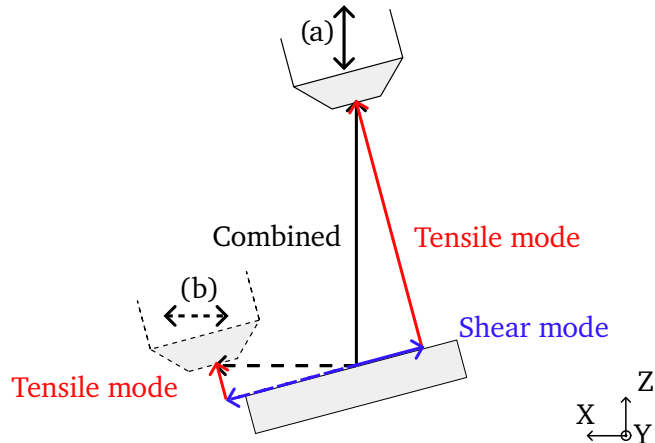


Figure 4.18: The shuttle is tilted inside the bath at  $15^\circ$ . Pulling on the sample in Z direction (a) results in mostly tensile stress and some shear stress on the sample. Pulling in X direction (b) results in mostly shear stress and some tensile stress.

Attempts of separating the ice layer by traversing in X and Z direction are compared. Less force was transferred when pulling in X direction. This is detected by the manually applied force to the stage. No separation or breaks are confirmed in those tests. This suggests that HFE is susceptible to shear forces. Therefore, detachment in Z-direction is more likely.

## Positioning

Before attaching the finger to the sample, the finger is positioned with the stages. At positioning, two different errors can occur: first, the finger is incorrectly positioned in X and Y direction over the sample. The HFE will spread partially on and under the window brace. The second error is a too small or too big gap between finger and sample in Z-direction.

An incorrectly position in X or Y direction is expected to massively effect detaching. Depending on the overlap, the force is transferred mostly to the window brace than to the sample. This will lead to an unsuccessful detachment. With the setup of a stage in each axis, the positioning is easily corrected. Under the tensile testing machine, a window brace with a bigger central hole makes positioning easier.

The gap between sample and finger is sometimes hard to estimate. The HFE volume influences the optimal gap size to avoid pressing the HFE between sample and window. On the other hand, HFE is shrinking between temperatures used at attaching and pulling. Also the cohesion of HFE is low, so keeping a bigger gap will also influence the maximum force. Therefore, the gap size is not completely isolatable with the HFE volume. As applying HFE is not achieved in a repeatable manner, the optimal gap distance is not defined.

## **observed error sources**

The duration of time between reaching the "glue" state from the "unglue" state makes disconnecting before pulling more likely. The sample is cooled with the finger on top as well as by the harbor cooled with liquid nitrogen. Best case is the same cooling rate of finger and harbor. In practice, the cooling of the finger is faster. This typically leads to a good connection. If for example major leaks occur in the cold nitrogen gas supply, the cooling rate of the finger is slower than the harbor. In those cases, the finger does not stay attached to the sample. A theory is that HFE gets more viscous on the sample than on the finger. While the HFE is perfectly adhering to the samples surface, the HFE loses volume due to cooling. The HFE on the tip is warmer and less viscous, being able to flow out of the gap to the sample due to gravity. Therefore, less adhesion to the finger tip is present.

In some experiments, high buildup of additional ice is observed on the sample. The buildup ice is looser, reducing the possible grip onto the desired ice layer. Therefore ice buildup should be avoided.

The formation of ice inside the bath is largely inhibited through the warm nitrogen gas outlets on the bath. The nitrogen is forming a barrier to the atmosphere which contains humidity that turns into ice at cold temperatures. However, through turbulence and the finger, some ice can form inside the bath. With some height and position correction or with a lid fitting onto the bath, ice buildup can be avoided

Another source of ice formation is traced back to a leakage in the finger. The tolerances between 3D printed part and metal bar should seal the gap airtight. But through changing out parts, the tolerances increased, allowing a weak cold nitrogen current leaking on the sample. As the cold gas itself is only nitrogen, there are two possibilities where the humidity itself is coming from: The cold nitrogen gas itself could contain some humidity. Second through additional turbulence, air is sucked through the nitrogen barrier. The air is directed onto the sample, causing more ice buildup. To avoid this, the gap is sealed tight with twinsil lubricating silicone typically used for dental applications.

### **4.2.7 Tensile testing of engineered layer with finger**

To lift off a piece of the ice layer, the ice layer must be broken in some way. thicker ice layers are expected to be harder to break than thinner ones due to the bigger cross section. Also amorphic vitrified ice is expected to be more stable than crystallized ice.

Initially, to save time for experiments, the samples are manually plunge-frozen in liquid nitrogen, as described before. However, the ice layers are less consistent compared to plunge freezing, resulting in mostly thicker ice layers. also as the sample is frozen in liquid nitrogen and with cover glass as sample holder, the leidenfrost effect is inhibiting the formation of vitrified ice.

First, the difference between plunge-freezer and manual process is verified with experiments. To compare plunge freezing by a plunge-freezer to the manual process, samples with lipid coated slides which are prepared with a plunge freezer and samples frozen manually are created. The water applied to form the ice layer is mixed with fluoresceine. The fluoresceine to water ratio is 50 mL/10 mg and 5 L/10mg, depending on the microscope setup and objectives.

Manual freezing shows a less predictable shaped ice layer. Formation of a non continuous layer (Fig. 4.19 (a) and (b)) and continuous layer is possible (Fig. 4.19 (c) and (d)). A plunge freezer reliably produces a continuous layer (Fig. 4.20). The thickness between samples varies. Some ice layers are thick enough to

include air bubbles. Also, both hand-freezed and plunge-freezed samples ice layer have sometimes visible cracks.

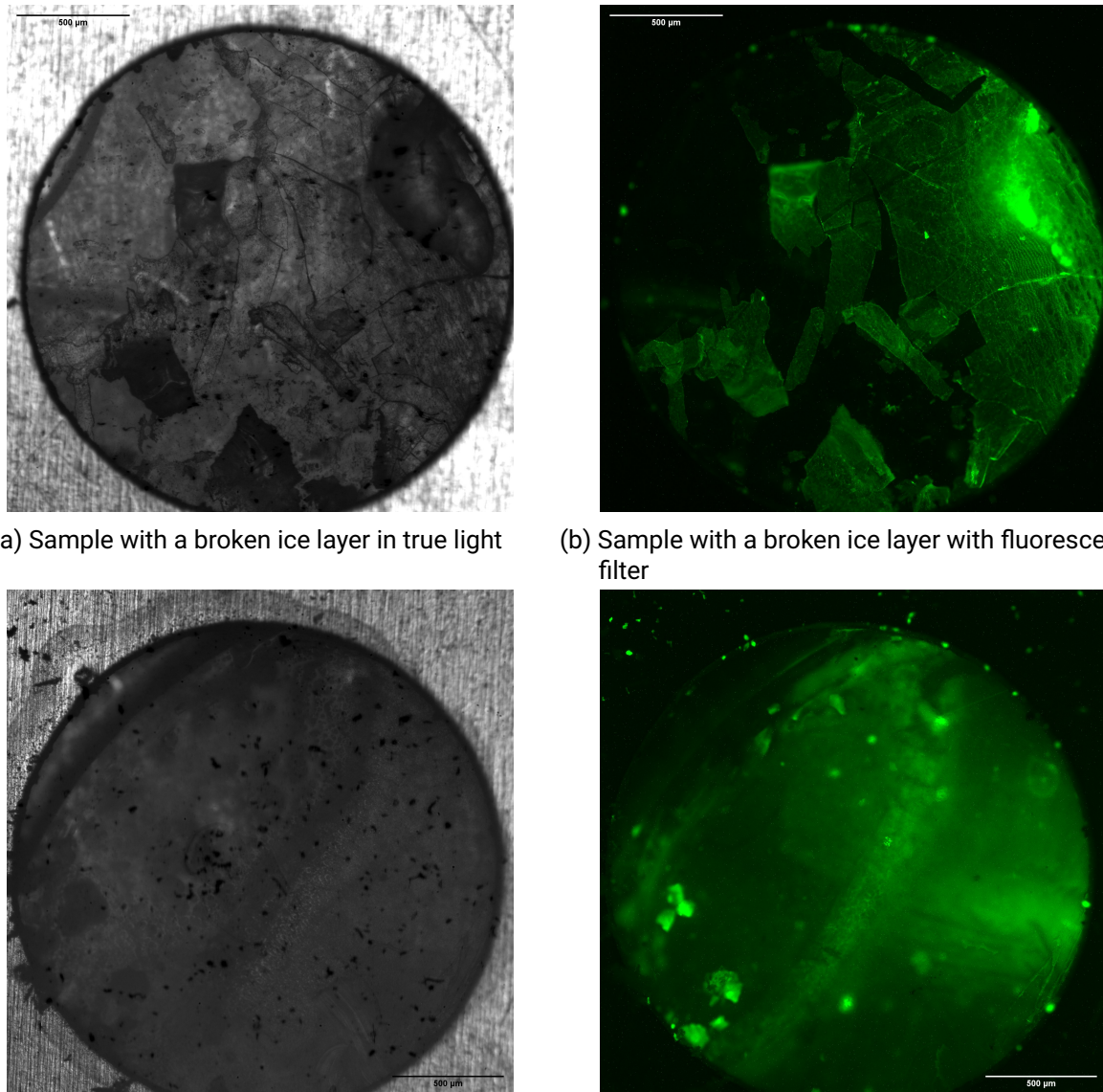


Figure 4.19: Two different examples for hand freezed ice layers on samples.

To further compare both methods, separation attempts with the finger are made at manually frozen and plunge-frozen samples. The results are categorized in 4 categories: Not successful pulls don't have visible changes of the fluorescent ice layer, Partially successes are visible breaks or clear movement of ice parts on the ice layer, Successful liftoff is a missing piece and a visible piece on the finger, which could be used for future steps.

In the results, there is no difference between manually frozen and plunge-frozen samples regarding detachability (Table 4.3). Therefore, using a plunge-freezer does not result in samples with favorable properties. manually frozen samples are also a good substitute for plunge freezing in future steps.

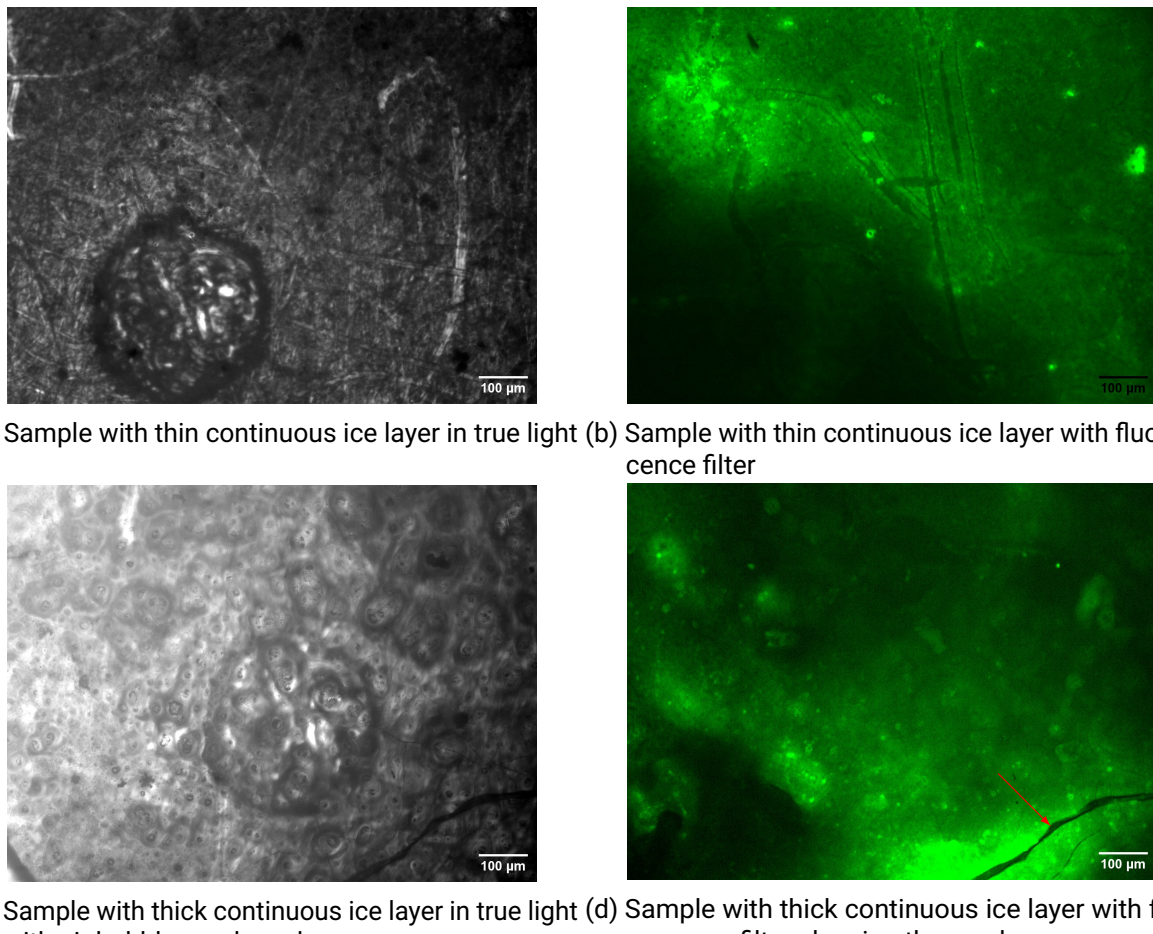


Figure 4.20: Two different examples for hand freezed ice layers on samples.

Now, different PDMS mixtures with plasma activation are tested. 4:1 with 10 min with plasma activation of 100 W over 10 min is used as reference. 50:1 mixture ratio is tested with different plasma activation duration. To verify the results of [12], PDMS with 50:1 mixture treated with 3 min at 100 W and 10 min at 100 W. For 1:2 mixture ratio, a minimum plasma activation of 30 W over 0.2 s and 35 W over 0.3 s are tested.

There are different mechanisms for each mixture ratio to decrease adhesion. 1:2 mixture ratio has low ice adhesion without additional treatment. The plasma activation is kept to a minimum to avoid inducing additional adhesion. At 50:1 mixture ratio, literature suggest that ice adhesion drops with increasing plasma treatment up to 90 % [12]. In 4:1 is a mixture ratio which potentially could combine the low ice adhesion without plasma treatment. The hope is that strong plasma treatment will induce brittleness and lower ice adhesion.

The finger requires a temperature of  $-160^{\circ}\text{C}$ . Therefore, the temperature drops enough to make PDMS of 10:1 mixture ratio brittle. Generally, a brittle PDMS surface helps to detach the ice layer. Tensile forces loosens the PDMS under the ice. The PDMS layer breaks within itself, loosening the ice layer from the rest of the sample. Still, an extreme brittleness is needed, which may not be reached. With PDMS of other mixture ratios, the brittleness could change, including the temperature dependency.

To compare PDMS coated sample holders to lipid coated sample holders, the same experiment is repeated

Category	Hand-freezed	Plunge-freezed
count executed tries	4	4
unsuccessful	3	3
breaks/movement of ice	1	1
piece lifted with finger	0	0

Table 4.3: Comparison of detachability between hand-frozen and plunge-frozen samples. Even with higher variabilities in hand-frozen samples, no difference in separation attempts are noticed.

Category	PDMS 1:2	PDMS 4:1	PDMS 50:1
count executed tries	5	3	6
unsuccessful	5	2	6
breaks/movement of ice	0	0	0
piece lifted with finger	0	1*	0

Table 4.4: Comparison of detachability between PDMS mixture ratios. Pulling tests at PDMS of 1:2 and 50:1 mixture ratio were unsuccessful. But at mixture ratio of 4:1, detachment was successful one time. A hole is visible on microscope, but as the specific region of the sample is not imaged before pulling, the creation of the hole by pulling cannot be verified, even if unlikely.

for three different mixture ratios. Under the microscope, a continuous layer of ice is visible. 4.21). The ice layer has the same structure for each mixture ratio. Still, the ice structure differs to ice frozen on lipid sample holders (Fig 4.19, 4.20). The layer is only interrupted by the imprint of pincers used at plunge freezing, visible in Fig. 4.21f. Also almost no cracks are visible in the ice layer. This indicates a strong continuous ice layer.

In pulling tests with the finger the three PDMS mixture ratios are tested. For mixture ratio 1:2 and 50:1, all test are unsuccessful (Table 4.4). however, at mixture ratio 4:1, a successful detachment was performed. However, the detachment cannot be confirmed as the before picture did not cover the area of the missing piece (Fig. 4.22). without this proof, the formation of the hole when freezing cannot ruled out even if unlikely. Also a piece of ice is not distinguishable when hanging on the finger. Still, since a mixture ratio gave the most promising results, this mixture ratio needs to be investigated further.

With the results in chapter 4.2.6, a separation in all PDMS Mixture ratios was expected. This is clearly not the case. Therefore different factors lead to an increase of tensile strength of the ice layer on PDMS. In 1:2 mixture ratio, additional adhesion resulting of increased wettability in plasma activation is mostly ignored. The ice layer could be generally thicker. Changes in microscope setup reduced visibility. Thick layers are more visible which could induce a bias by sorting out thin less visible ice layers. Also the Ice layer is continuous, which could make breaking off a piece of ice harder or guide forces over a larger area. The last theory is tested by damaging the ice surface.

To test the behavior of an ice layer frozen onto PDMS, the surface is damaged in two ways: In one experiment, samples of 1:2 and 50:1 are scratched with a diamond pencil. This is done after mounting the sample on the shuttle. The diamond tip is drawn around the inside of the window several times.

Scratching the ice layer with a diamond pencil leaves a visible groove in the ice layer (Fig. 4.23). The ice surface is clearly damaged by the groove. Still, no additional cracks appear. Also separation attempts with the finger were unsuccessful. Therefore, the ice layer itself is still sticking to the PDMS. Therefore the adhesion to PDMS itself is probably increased.

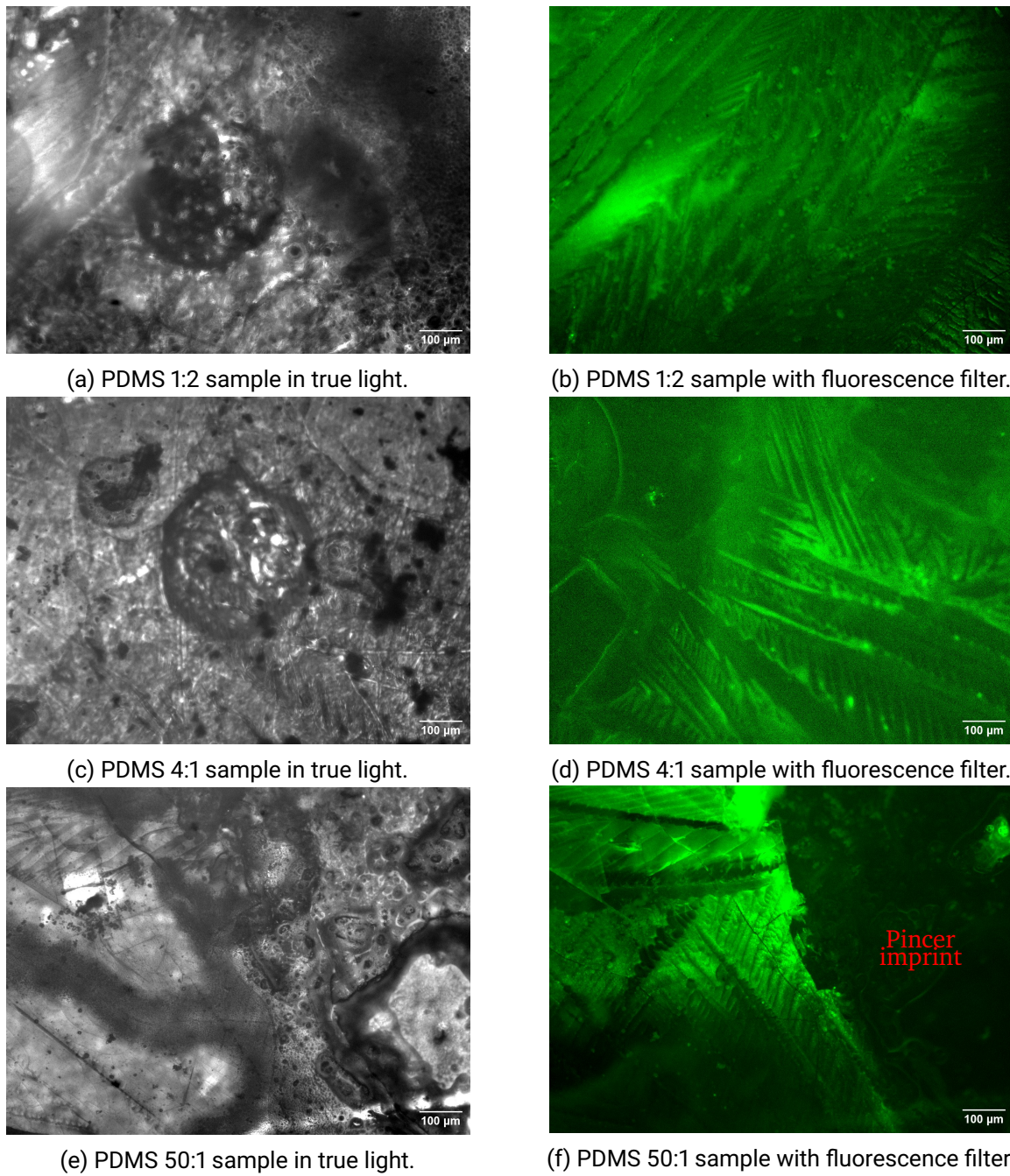
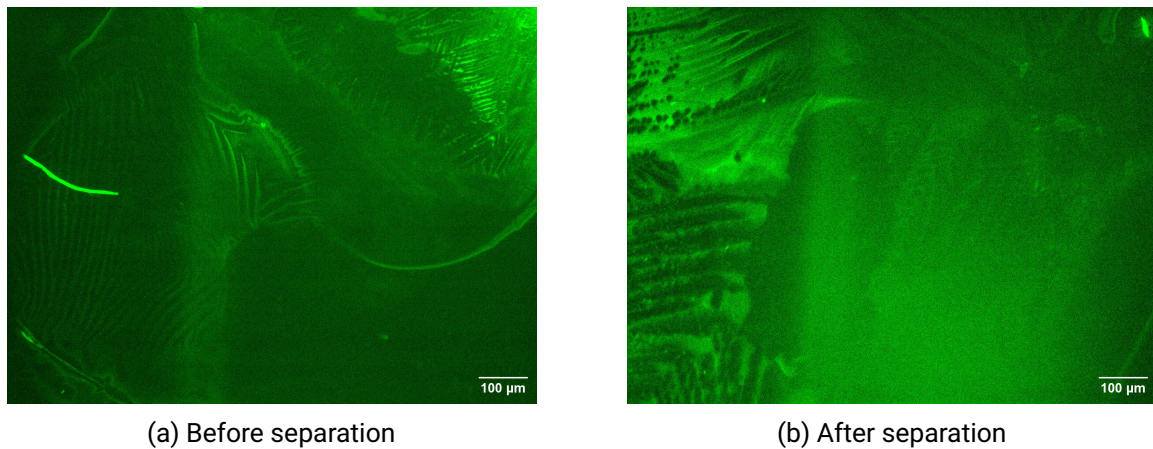


Figure 4.21: comparison of ice on different PDMS samples. The ice crystallized ice structure only changes minimally. A continuous ice layer forms over each plasma activated PDMS sample. the layer is only interrupted by the imprint of the pinces at plunge-freezing here visible in (f).

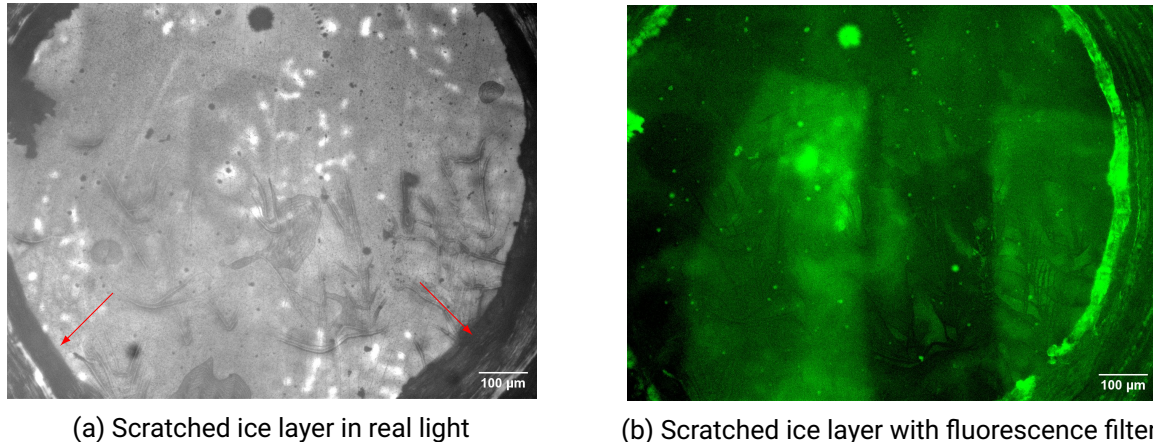
In another experiment, the pincer is intentionally placed through the middle of 1:2 PDMS coated sample holder when plunge-freezing. Therefore an intentional big imprint is left after freezing. The effect of plasma treatment gets reversed in places the sample holder is touched with the pincer. The pincer gets stuck in the ice layer when frozen. When the pincer is detached, a big imprint is left with some tiny loose ice pieces (Fig. 4.24). In separation attempts, these loose ice pieces is moved by the finger. Additionally, cracks appeared



(a) Before separation

(b) After separation

Figure 4.22: Successful pulling test of 4:1 mixture ratio PDMS. However, this result should be taken cautiously. The before and after image each catch a different part of the sample. Under normal circumstances, no holes form in the ice layer when freezing (shown in Fig. 4.21) however, as the area is not visible in the before image, this case cannot be ruled out.

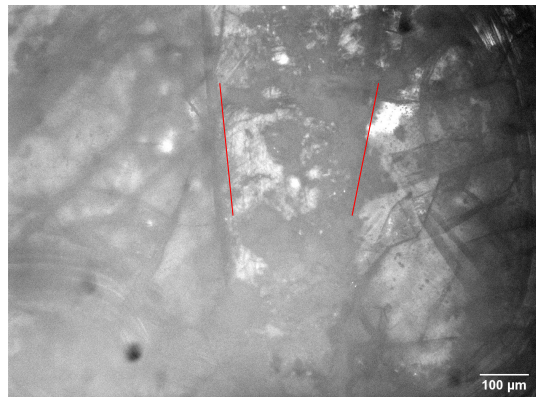


(a) Scratched ice layer in real light

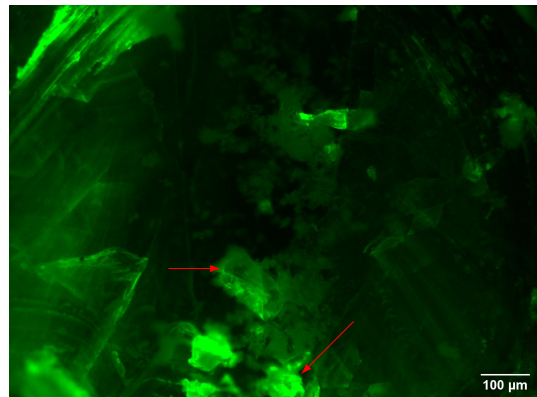
(b) Scratched ice layer with fluorescence filter.

Figure 4.23: Ice layer scratched with diamond pencil. in (b), the mirrored F-shape mark is visible through the thin ice. This mark shows which side is PDMS coated in fabrication, as the PDMS is transparent. No cracks formed, suggesting the ice is firmly bound to the PDMS. Also separation attempts were unsuccessful.

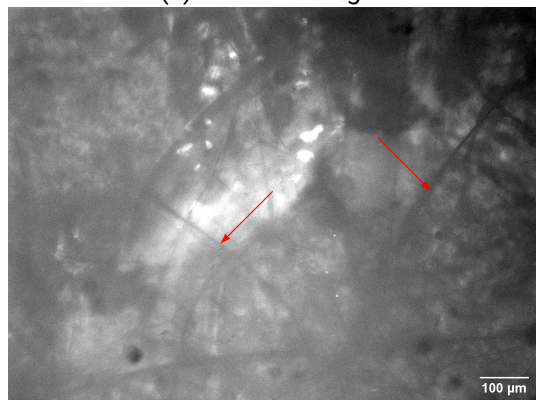
after pulling. This suggest that intentionally damaging or modifying the surface after plasma activation could reduce ice adhesion and makes separation easier.



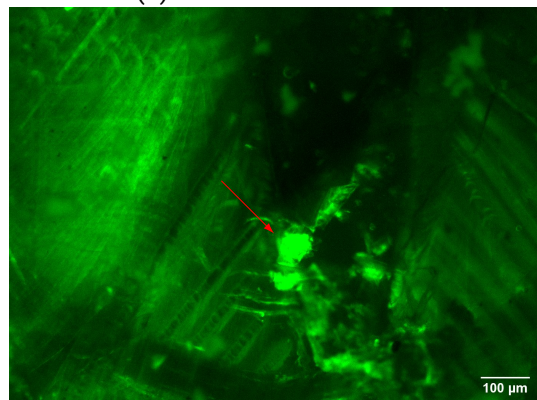
(a) Before real light



(b) Before fluorescence



(c) After real light



(d) After fluorescence

Figure 4.24: Ice layer on 1:2 PDMS with loose ice near pincer imprint. The Imprint is shown in (a). The finger is able to move the loose ice crystals, which is visible in (b) and (c). Also new cracks are formed in (c).

## 5 Conclusion and Outlook

---

In conclusion, no solvent was found with high enough solubility to dissolve a lipid layer at cryogenic temperatures. Results show that solvents used for lipids are generally endothermic. Some solubility is reached at cryogenic temperature, but not enough to completely dissolve a lipid layer. Finding a solvent by chance is unlikely, as dissolving processes of lipids are majorly endothermic and therefore show low performance at cryogenic temperatures.

The potential for lipids and detergents is not exhausted in this thesis. To engineer a sacrificial layer, other detergents could be used [22]. An exothermic process is also not limited through the cyrogenic temperatures. Alternatively, to increase solubility, changing the pH value of lipid and solvent could increase solubility [23].

PDMS is tuned at room temperature. Results have confirmed a connection between adhesion forces measured in papers and at tensile testing. Plasma activation has the opposite effect of 1:2 mixture ratio than on 50:1 mixture ratio. The surface gets more stable with increasing plasma activation instead of more brittle.

At cryogenic temperatures, a successful separation was made with 4:1 mixture ratio PDMS. A hole was observed suggesting a detachment. But the repeatability must be shown in future work, since limited tests are done with 4:1 mixture ratio.

All PDMS coated sample holders resulted in a continuous ice layers without cracks. PDMS of 1:2 with minimal plasma activation and 50:1 with high plasma activation resulted in ice layers which are not separable. No separation attempt was successful for both mixture ratio.

In contrast to PDMS coated sample holders, lipid coated sample holders resulted in cracks in the ice layer itself. In pulling tests with the finger, breaking and moving parts of the ice layer were possible in 1 out of 4 cases. To help detach the lipid layer, PDMS could be used. With increased brittleness and pre-broken ice layer, less stress is needed for detaching.

A combination of lipids and PDMS could be attempted. The brittleness of HFE and the cracks in the ice layer resulting from lipids could help decrease adhesion for a reliable detachment.

The finger with HFE is able to apply tensile stress between 103.3 kPa and 585.4 kPa. The stress applied is a couple magnitude higher than the stress calculated for detaching PDMS. As no detachment was made, additional factors increase tensile stress needed for detachment. The discrepancy could be result of energy lost deforming HFE at cryogenic temperatures, stability of a continuous ice layer, as well as the effect of plasma activation on some mixture ratios.

Different factors which increase and decrease the effectiveness of the finger: Too much HFE results in HFE ripping because of the low cohesion. Too little HFE is prone to not properly attaching to the Sample. lower temperature increase the viscosity and therefore stability of HFE. But at around  $-170^{\circ}\text{C}$ , cracks form in HFE and the strength is drastically reduced.

The direction of force could help at detaching an ice layer. However, the observed stability to shear load of HFE is considerably lower than tensile load.

Positioning is also important, especially keeping the correct gap between sample and finger in which the HFE is spread thin but not flows between window and sample. Also slow temperature changes are drastically reducing the likelihood of a good connection between sample and finger.

The force applied with the finger is not able to reliably break the ice layer on the sample. Pre-broken ice pieces are often picked up. A process is needed to completely loosen the ice layer without the "finger". For example, deactivating the plasma by putting a grid on the PDMS after Plasma activation could result in a loose, non-continuous but regular layer. Smaller pieces with less adhesion are easier to detach.

In general, the finger setup turned out to be not reliable. Even after analysis, forces applied with the finger vary too much for inducing strong forces to a sample. However, pre-broken pieces may be able to be picked up easier. Therefore, other methods of breaking loose the ice layer should be searched.

Another way to create a loose ice layer is to engineer the ice layer itself. Additives inside the ice layer could help in the breaking process. Freezing the ice in an emulsion could result in an in-continuous ice layer.

## 6 References

---

- [1] Rainer Heintzmann and Gabriella Ficz. “Breaking the resolution limit in light microscopy”. In: *Briefings in functional genomics & proteomics* 5.4 (2006), pp. 289–301. issn: 1473-9550. doi: 10.1093/bfgp/e11036.
- [2] Brian Wowk. “Thermodynamic aspects of vitrification”. In: *Cryobiology* 60.1 (2010), pp. 11–22. issn: 0011-2240. doi: 10.1016/j.cryobiol.2009.05.007. url: <https://www.sciencedirect.com/science/article/pii/S0011224009000674>.
- [3] Dganit Danino. “Cryo-TEM of soft molecular assemblies”. In: *Current Opinion in Colloid & Interface Science* 17.6 (2012), pp. 316–329. issn: 1359-0294. doi: 10.1016/j.cocis.2012.10.003. url: <https://www.sciencedirect.com/science/article/pii/S1359029412001033>.
- [4] R. Faoro, M. Bassu, and T. P. Burg. “Determination of the refractive index of liquids at cryogenic temperature”. In: *Applied Physics Letters* 113.8 (2018), p. 081903. issn: 0003-6951. doi: 10.1063/1.5043370.
- [5] Lasse Makkonen. “Ice Adhesion —Theory, Measurements and Countermeasures”. In: *Journal of Adhesion Science and Technology* 26.4-5 (2012), pp. 413–445. issn: 0169-4243. doi: 10.1163/016942411X574583. url: [https://www.researchgate.net/publication/254214058\\_Ice\\_Adhesion\\_-Theory\\_Measurements\\_and\\_Countermeasures](https://www.researchgate.net/publication/254214058_Ice_Adhesion_-Theory_Measurements_and_Countermeasures).
- [6] Siyan Yang et al. “Condensation frosting and passive anti-frosting”. In: *Cell Reports Physical Science* 2.7 (2021), p. 100474. issn: 2666-3864. doi: 10.1016/j.xcrp.2021.100474. url: <https://www.sciencedirect.com/science/article/pii/S2666386421001740>.
- [7] Marc P. Wolf, Georgette B. Salieb-Beugelaar, and Patrick Hunziker. “PDMS with designer functionalities—Properties, modifications strategies, and applications”. In: *Progress in Polymer Science* 83 (2018), pp. 97–134. issn: 0079-6700. doi: 10.1016/j.progpolymsci.2018.06.001. url: <https://www.sciencedirect.com/science/article/pii/S0079670017300783>.
- [8] Junpeng Liu et al. “Development and evaluation of poly(dimethylsiloxane) based composite coatings for icephobic applications”. In: *Surface and Coatings Technology* 349 (2018), pp. 980–985. issn: 02578972. doi: 10.1016/j.surfcoat.2018.06.066. url: <https://www.sciencedirect.com/science/article/pii/S025789721830642X>.
- [9] DOW. *Datasheet SYLGARD™ 184 Silicone Elastomer*. Ed. by DOW.
- [10] Pablo F. Ibáñez-Ibáñez et al. “Ice adhesion of PDMS surfaces with balanced elastic and water-repellent properties”. In: *Journal of Colloid and Interface Science* 608.Pt 1 (2022), pp. 792–799. issn: 0021-9797. doi: 10.1016/j.jcis.2021.10.005. url: <https://www.sciencedirect.com/science/article/pii/S0021979721016714>.
- [11] Michael J. Owen and Patrick J. Smith. “Plasma treatment of polydimethylsiloxane”. In: *Journal of Adhesion Science and Technology* 8.10 (1994), pp. 1063–1075. issn: 0169-4243. doi: 10.1163/156856194X00942.

- [12] Taiki Ohishi et al. “Tensile strength of oxygen plasma-created surface layer of PDMS”. In: *Journal of Micromechanics and Microengineering* 27.1 (2017), p. 015015. ISSN: 0960-1317. doi: 10.1088/0960-1317/27/1/015015.
- [13] Srirama M. Bhairi, Ph. D. “Detergents: A guide to the properties and uses of detergents in biology and biochemistry”. In: (2001), pp. 6–7.
- [14] comelec. *Parylene Coatings*. Ed. by comelec. URL: <https://comelec.ch/parylene-coatings/>.
- [15] Mark Tye Zafir Javeed. *Enthalpy of Solution*. URL: [https://chem.libretexts.org/Bookshelves/Physical\\_and\\_Theoretical\\_Chemistry\\_Textbook\\_Maps/Supplemental\\_Modules\\_\(Physical\\_and\\_Theoretical\\_Chemistry\)/Physical\\_Properties\\_of\\_Matter/Solutions\\_and\\_Mixtures/Solution\\_Basics/Enthalpy\\_of\\_Solution](https://chem.libretexts.org/Bookshelves/Physical_and_Theoretical_Chemistry_Textbook_Maps/Supplemental_Modules_(Physical_and_Theoretical_Chemistry)/Physical_Properties_of_Matter/Solutions_and_Mixtures/Solution_Basics/Enthalpy_of_Solution).
- [16] Charles E. Mortimer and Ulrich Müller. *Chemie: Das Basiswissen der Chemie ; 126 Tabellen*. 9., überarb. Aufl. Stuttgart: Thieme, 2007. ISBN: 9783134843095. URL: [https://books.google.de/books?id=kf\\_1FH8Le6QC](https://books.google.de/books?id=kf_1FH8Le6QC).
- [17] R Wayne Albers. “Phospholipid Bilayers”. In: *Basic Neurochemistry: Molecular, Cellular and Medical Aspects. 6th edition*. Ed. by R. Wayne Albers. Lippincott-Raven, 1999. URL: <https://www.ncbi.nlm.nih.gov/books/NBK28248/>.
- [18] PubChem. *Ethane*. 2023. URL: <https://pubchem.ncbi.nlm.nih.gov/compound/Ethane> (visited on 08/29/2023).
- [19] Wen-Tien Tsai. “Environmental risk assessment of hydrofluoroethers (HFEs)”. In: *Journal of Hazardous Materials* 119.1-3 (2005), pp. 69–78. ISSN: 0304-3894. doi: 10.1016/j.jhazmat.2004.12.018. URL: <https://www.sciencedirect.com/science/article/pii/S0304389404006466>.
- [20] Raffaele Faoro et al. “Aberration-corrected cryoimmersion light microscopy”. In: *Proceedings of the National Academy of Sciences of the United States of America* 115.6 (2018), pp. 1204–1209. doi: 10.1073/pnas.1717282115.
- [21] Guiguan Zhang et al. “Experimental study on mechanical performance of polydimethylsiloxane (PDMS) at various temperatures”. In: *Polymer Testing* 90 (2020), p. 106670. ISSN: 01429418. doi: 10.1016/j.polymertesting.2020.106670.
- [22] Sigma-Aldrich. *Safety data sheet HFE 7200*. Ed. by Sigma-Aldrich. 2023.
- [23] Bruce A. Averill, Patricia Eldredge. *Principles of General Chemistry: Solubility and pH*. URL: <https://2012books.lardbucket.org/books/principles-of-general-chemistry-v1.0/s21-04-solubility-and-ph.html>.